

# FAST PARALLEL VOLUME VISUALIZATION ON CUDA TECHNOLOGY

ADESHINA ADEKUNLE MICHEAL

A thesis submitted in  
fulfilment of the requirement for the award of the  
Doctor of Philosophy

Faculty of Computer Science and Information Technology  
Universiti Tun Hussein Onn Malaysia

November 2013

## ABSTRACT

In the medical diagnosis and treatment planning, radiologists and surgeons rely heavily on the slices produced by medical imaging scanners. Unfortunately, most of these scanners can only produce two dimensional images because the machines that can produce three dimensional are very expensive. The two dimensional images from these devices are difficult to interpret because they only show cross-sectional views of the human structure. Consequently, such circumstances require highly qualified doctors to use their expertise in the interpretation of the possible location, size or shape of the abnormalities especially for large datasets of enormous amount of slices. Previously, the concept of reconstructing two dimensional images to three dimensional was introduced. However, such reconstruction model requires high performance computation, may either be time-consuming or costly. Furthermore, detecting the internal features of human anatomical structure, such as the imaging of the blood vessels, is still an open topic in the computer-aided diagnosis of disorders and pathologies. This study proposed, designed and implemented a visualization framework named *SurLens* with high performance computing using Compute Unified Device Architecture (CUDA), augmenting the widely proven ray casting technique in terms of superior qualities of images but with slow speed. Considering the rapid development of technology in the medical community, our framework is implemented on Microsoft .NET environment for easy interoperability with other emerging revolutionary tools. The Visualization System was evaluated with brain datasets from the department of Surgery, University of North Carolina, United States, containing 109 datasets of MRA, T1-FLASH, T2-Weighted, DTI and T1-MPRAGE. Significantly, at a reasonably cheaper cost, *SurLens* Visualization System achieves immediate reconstruction and obvious mappings of the internal features of the human brain, reliable enough for instantaneously locate possible blockages in the brain blood vessels without any prior segmentation of the datasets.

## ABSTRAK

Dalam diagnosis perubatan dan perancangan rawatan, pakar radiologi dan pakar bedah bergantung pada hirisan yang dihasilkan oleh pengimbas pengimejan perubatan. Malangnya, kini kebanyakan pengimbas hanya boleh menghasilkan imej dua dimensi. Mesin yang dapat menghasilkan imej tiga dimensi adalah terlalu mahal. Imej dua dimensi yang terhasil ini adalah sukar untuk ditafsir kerana mereka hanya menunjukkan pandangan keratan rentas struktur manusia. Oleh itu, keadaan seperti ini memerlukan doktor pakar untuk menggunakan pengalaman mereka dalam tafsiran lokasi, saiz atau bentuk keabnormalan terutama sekali untuk set data yang besar. Sebelum ini, konsep membina semula imej dua dimensi ke tiga dimensi diperkenalkan. Walau bagaimanapun, model penyusunan semula itu memerlukan pengiraan berprestasi tinggi, sama ada memakan masa atau kos yang tinggi. Tambahan pula, mengesan ciri-ciri dalaman struktur anatomi manusia, seperti pengimejan saluran darah merupakan topik yang masih hangat dalam diagnosis berbantu komputer dan pathologi. Kajian ini mencadangkan, mereka bentuk dan melaksanakan rangka kerja visualisasi dinamakan *SurLens* dengan high performance computing menggunakan Compute Unified Device Architecture (CUDA) menggunakan platform Microsoft.NET. Sistem Visualisasi ini telah divalidasi dengan menggunakan dataset daripada jabatan Pembedahan, Universiti North Carolina, Amerika Syarikat, yang mengandungi 109 dataset dari jenis MRA, T1-FLASH, T2 Berwajaran, DTI dan T1-MPRAGE. Pada kos yang rendah, *SurLens* Sistem Visualisasi mencapai pembinaan semula serta-merta dan pemetaan jelas ciri-ciri dalaman otak manusia dengan kebolehpercayaan yang tinggi untuk menentukan lokasi kemungkinan berlaku sumbatan pada saluran darah otak tanpa perlu disegmentasi terlebih dahulu.

## CONTENTS

<b>TITLE</b>	<b>i</b>
<b>DECLARATION</b>	<b>ii</b>
<b>DEDICATION</b>	<b>iii</b>
<b>ACKNOWLEDGMENT</b>	<b>iv</b>
<b>ABSTRACT</b>	<b>v</b>
<b>LIST OF PUBLICATIONS</b>	<b>vii</b>
<b>CONTENTS</b>	<b>ix</b>
<b>LIST OF TABLES</b>	<b>xiv</b>
<b>LIST OF FIGURES</b>	<b>xv</b>
<b>LIST OF SYMBOLS AND ABBREVIATIONS</b>	<b>xix</b>
<b>LIST OF APPENDICES</b>	<b>xxiv</b>
 <b>CHAPTER 1 INTRODUCTION</b>	
1.1 Background Study	1
1.2 Brain Anatomy and Abnormalities	2
1.3 Motivation	4
1.4 Research Questions	7
1.5 Research Objectives	7
1.6 Scope of the Research	8
1.7 Organization of the Thesis	8

## CHAPTER 2 VISUALIZATION OF VOLUMETRIC DATASETS

2.1	Introduction	10
2.2	Volume Visualization	12
2.3	Volumetric Image Datasets	13
2.4	Medical Imaging Modalities	16
2.4.1	Computed Tomography	17
2.4.2	Magnetic Resonance Imaging	18
2.4.3	Clinical Applications / Relevancies	20
2.5	Dataset Pre-Processing Techniques	21
2.5.1	Filtering, Enhancement, Detection& Extraction	21
2.5.2	Volume Segmentation	23
2.5.3	Data Reduction	25
2.6	Medical Volume Visualization	26
2.6.1	Volumetric Image Visualization	27
2.6.2	Multipanar Reformation (MPR)	28
2.6.3	Surface Rendering Technique	29
2.6.4	Direct Rendering Technique	30
2.6.5	3-D Reconstruction	31
2.7	CUDA Technology	32
2.8	Software Components	36
2.8.1	Graphics Execution	37
2.8.2	Volume Rendering	39
	2.8.2.1 Classification	40
	2.8.2.2 Rendering	42
2.9	Frameworks in Medical Volume Visualization	43
2.9.1	Probe-Volume: An Exploratory Volume Visualization Framework	45
2.9.2	VDVR: Verifiable Visualization of Projection-Based Data	46

2.9.3	GPU Accelerated Generation of Digitally Reconstructed Radiographs for 2-D / 3-D Image Registration	48
2.9.4	Volume Visualization with Grid-Independent Adaptive Monte Carlo Sampling	48
2.9.5	Framework for Volume Segmentation, Visualization using Augmented Reality	49
2.9.6	Illustrative Volume Visualization using GPU-Based Particle Systems	50
2.9.7	Volumetric Ambient Occlusion for Real-Time Rendering and Games	51
2.9.8	An Improved Volume Rendering Algorithm Based on Voxel Segmentation	52
2.9.9	ParaView Visualization Framework	53
2.9.10	VolView Framework	54
2.10	Advantages & Disadvantages of Previous Frameworks	55
2.11	Summary	59

### **CHAPTER 3 METHODOLOGY: THE DEVELOPMENT OF *SurLens***

3.1	Introduction	62
3.2	SurLens Architecture	63
3.3	The Framework of SurLens	65
3.3.1	Datasets Pre-Processing	68
3.3.1.1	Application of Projective Plane Theorem	68
3.3.1.2	Coordinates Systems	74
3.3.1.3	Intensity Matching	81
3.3.2	Accelerating Hardware	83
3.3.2.1	Data Structuring & Fragmentation	85
3.3.3	Graphic Execution Phase	89

3.3.4	Volume Rendering Phase	90
3.3.4.1	Camera Model	91
3.3.4.2	Volume Classification	93
3.3.4.3	Shading and Gradient Computation	95
3.3.4.4	Interpolation / Re-sampling	97
3.3.4.5	Compositing	98
3.4	Summary	102

## **CHAPTER 4 IMPLEMENTATION AND TEST DATASETS**

4.1	Introduction	104
4.2	Conversion Scheme	108
4.3	Feature & Edge Detection Scheme	112
4.4	Automatic Feature & Mapping Technique	115
4.5	SurLens Robust Algorithms' for Mass data	119
4.6	Summary	120

## **CHAPTER 5 RESULTS AND DISCUSSION**

5.1	Introduction	122
5.2	Results of New Feature & Edge Detection Scheme	123
5.2.1	Experimentation with MRA Datasets	124
5.2.2	Experimentation with DTI Datasets	126
5.2.3	Experimentation with T1-FLASH Datasets	128
5.2.4	Experimentation with T1-MPRAGE Datasets	129
5.3	Results of New Feature Mapping Techniques	130
5.3.1	Experimentation with MRA Datasets	131
5.3.2	Experimentation with DTI Datasets	142
5.3.3	Experimentation with T1-FLASH Datasets	145
5.3.4	Experimentation with T1-MPRAGE Datasets	147
5.4	SurLens Comparison with other Visualization Systems	149

5.4.1	ParaView & VolView Visualization Systems	149
5.5	Results of Robust Algorithms for Mass data	154
5.5.1	Speed Evaluation with MRA Datasets	155
5.5.2	Speed Evaluation with DTI Datasets	159
5.5.3	Speed Evaluation with T1-FLASH Dataset	160
5.5.4	Speed Evaluation with T1-MPRAGE Dataset	161
5.6	Summary	162
<b>CHAPTER 6 CONCLUSION</b>		
6.1.	Introduction	164
6.2.	Conclusion	165
6.3.	Contributions	169
6.4.	Future Works	170
<b>REFERENCES</b>		171
<b>APPENDIX A</b>		195
<b>APPENDIX B</b>		214
<b>VITA</b>		



**LIST OF TABLES**

2.1	Comparison of CPU and GPU	32
3.1	Homogeneous Coordinates Representation of Points and Lines	73
3.2	<i>SurLens</i> Access Design to Intensity	82
4.1	Experimental Testbeds	107
5.1	MRA Speed Evaluation for Datasets of Patient_001 to Patient_009	155
5.2	MRA Speed Evaluation for Datasets of Patient_010 to Patient_015	156
5.3	MRA Speed Evaluation for Datasets of Patient_016 to Patient_020	157
5.4	Randomly Selected Patients MRA Datasets for Speed Evaluation	158
5.5	Speed Evaluation for Selected Patients DTI Datasets	159
5.6	Speed Evaluation for Selected Patients T1-FLASH Datasets	160
5.7	Speed Evaluation for Selected Patients T1-MPRAGE Datasets	161

## LIST OF FIGURES

1.1	Conventional pathologists' slides viewing microscope	5
1.2	Clinical support with visualization	5
2.1	Volumetric Data in Cartesian Grid	15
2.2	Data Structure Grids	16
2.3	An example of a CT slice, a head scan	18
2.4	An example of an MRI slice, brain's Scan	20
2.5	VDVR Pipeline	47
2.6	The GPGPU Paradigm	50
3.1	<i>SurLens</i> Architecture	64
3.2	<i>SurLens</i> Framework Overview	66
3.3	<i>SurLens</i> Framework Phases	67
3.4	Parallel Lines in Projective Plane	69
3.5	Point Estimation of 2-D Slices	70
3.6	Translation	75
3.7	Scaling about the Origin	77
3.8	Rotation about x-axis	77
3.9	Rotation about y-axis	78
3.10	Rotation about z-axis	79
3.11	Algorithm 1: <i>SurLens</i> Algorithm for Dataset Pre-Processing	81
3.12	Algorithm 2: <i>SurLens</i> Algorithm for Accelerating Hardware	82
3.13	<i>SurLens</i> -CUDA Architecture	84
3.14	<i>SurLens</i> Data Fragmentation Procedures	87
3.15	<i>SurLens</i> Memory System Architecture	88
3.16	<i>SurLens</i> Graphic Execution Phase (Phase 3)	89
3.17	Algorithm 3: <i>SurLens</i> Algorithm for Graphic Execution	89
3.18	<i>SurLens</i> Volume Rendering Phase (Phase 4)	91
3.19	Image Point Processing Approach	93

3.20	Ambient Lighting	95
3.21	Diffuse Lighting	96
3.22	Specular Lighting	96
3.23	Absorption and Emission along Light Rays	100
3.24	Algorithm 4: <i>SurLens</i> Algorithm for Volume Rendering	102
4.1	<i>SurLens</i> Conversion Scheme	108
4.2	<i>SurLens</i> Conversion Scheme: Design Pipeline for Data Array Structure	109
4.3	<i>SurLens</i> Conversion Scheme: Design Pipeline for ImageData	110
4.4	<i>SurLens</i> Conversion Scheme: Design Pipeline of PointSet	111
4.5	Design of Contour Class for <i>SurLens</i> Feature & Edge Detection Scheme	112
4.6	Design of Anaglyph and Buffering Class for <i>SurLens</i> Feature & Edge Detection Scheme	113
4.7	Overview of <i>SurLens</i> Automatic Feature Mapping Techniques	116
4.8-a	<i>SurLens</i> Automatic Feature Mapping Techniques	116
4.8-b	<i>SurLens</i> Automatic Feature Mapping Techniques	117
5.1-a	Results of <i>SurLens</i> Feature & Edge Detection with MRA Datasets	124
5.1-b	Results of <i>SurLens</i> Feature & Edge Detection with MRA Datasets	125
5.2-a	Results of <i>SurLens</i> Feature & Edge Detection with DTI Datasets	126
5.2-b	Results of <i>SurLens</i> Feature & Edge Detection with DTI Datasets	127
5.3-a	Results of <i>SurLens</i> Feature & Edge Detection with T1-FLASH Datasets	128
5.3-b	Results of <i>SurLens</i> Feature & Edge Detection with T1-FLASH Datasets	129
5.4-a	Results of <i>SurLens</i> Feature & Edge Detection with T1-MPRAGE Datasets	130
5.4-b	Results of <i>SurLens</i> Feature & Edge Detection with T1-MPRAGE Datasets	130
5.5	MRA Evaluation Datasets of Patient_001 and Patient_002	132
5.6.	MRA Evaluation Datasets of Patient_003 and Patient_004	132
5.7.	MRA Evaluation Datasets of Patient_005	133
5.8.	MRA Evaluation Datasets of Patient_006	133
5.9.	MRA Evaluation Datasets of Patient_007 and Patient_009	134

5.10.	MRA Evaluation Datasets of Patient_010	135
5.11.	MRA Evaluation Datasets of Patient_011 and Patient_013	135
5.12-a	MRA Evaluation Datasets of Patient_014 and Patient_016	136
5.12-b	MRA Evaluation Datasets of Patient_014 and Patient_016	136
5.13.	MRA Evaluation Datasets of Patient_017	137
5.14	MRA Evaluation Datasets of Patient_018 and Patient_019	137
5.15.	MRA Evaluation Datasets of Patient_020 and Patient_027	138
5.16.	Randomly Selected Patient MRA Evaluation Datasets	138
5.17.	MRA Evaluation Datasets of Patient_048	139
5.18.	MRA Evaluation Datasets of Patient_052 and Patient_054	140
5.19.	MRA Evaluation Datasets of Patient_061 and Patient_067	140
5.20-a.	MRA Evaluation Datasets of Patient_073	140
5.20-b.	MRA Evaluation Datasets of Patient_077 and Patient_083	141
5.21.	MRA Evaluation Datasets of Patient_097	141
5.22.	MRA Evaluation Datasets of Patient_098	142
5.23.	DTI-Patient_067-Normal, Female, 57yrs	143
5.24.	DTI-Patient_098-Abnormal, Female, 54yrs	143
5.25.	DTI-Patient_054-Normal, Female, 34yrs	144
5.26.	DTI-Patient_047-Abnormal, Female, 31yrs	144
5.27.	T1-FLASH-Patient_067-Normal, Female, 57yrs	145
5.28.	T1-FLASH-Patient_054-Normal, Female, 34yrs	145
5.29.	T1-FLASH-Patient_047-Abnormal, Female, 31yrs	146
5.30.	Patient_099-Stripped-FLASH (Normal Patient)	146
5.31.	T1-MPRAGE-Patient_054, Normal, Female, 34yrs	147
5.32.	T1-MPRAGE-Patient_047, Abnormal, Female, 34yrs	147
5.33.	T1-MPRAGE-Patient_084, Abnormal, Female, 67yrs	148
5.34.	Comparison-Patient_097-MRA Datasets	151
5.35.	Comparison-Patient_054-MRA Datasets	151
5.36.	Comparison-Patient_098-DTI Datasets	152
5.37.	Comparison-Patient_084-T1-MPRAGE Datasets	152

5.38.	Comparison-Patient_099-Stripped_FLASH Datasets	153
5.39.	Divert Comparison-Patient_01_CT_Abdominal Pelvic Datasets	154

## LIST OF SYMBOLS AND ABBREVIATIONS

$\lambda$ -	Scale Factor
$f : \mathbf{E}^3 \rightarrow \mathfrak{R};$ -	Scalar Function
$f^n : \mathbf{E}^3 \rightarrow \mathfrak{R}^n$ -	n-Dimensional Vector Function
$f^{n^k} : \mathbf{E}^3 \rightarrow \mathfrak{R}^{n^k},$ -	A k-Ranked Tensor Function
$\pi$ -	Plane
$\pi'$ -	New plane
$(S_{k-1}, S_k)$ -	Optical Depth
$\tau$ -	Extinction Coefficient
$[X, Y, Z]^T$ -	Vector Notation
2-D -	Two Dimensional
3-D -	Three Dimensional
ANN -	Artificial Neural Networks
ANSI -	American National Standard Institute
AOH -	Application Oriented Hypothesis
API -	Application Programming Interface
AR -	Augmented Reality
B -	Strength of the Magnetic (field in tesla)
BCC -	Body Centered Cubic
C# -	C-Sharp
CAD -	Computer-Aided Design
Cg -	C for Graphics
CIL -	Common Intermediate Language
$\text{Cos}_\alpha$ -	Product of the Vector of Light Source (a negative value)
CPU -	Central Processing Unit
CRT -	Cathode Ray Tube
CT -	Computed Tomography

CTF -	Contrast Transfer Function
CUDA -	Compute Unified Device Architecture
$da$ -	normal
DDR -	Double Data Rates
DLL -	Dynamic-Link Library
DoD -	Department of Defense
DTI -	Diffusion Tensor Imaging
DVR -	Direct Volume Rendering
$d\Omega$ -	Solid Angle
FCM -	Fuzzy C-means
FDA -	Federal Drug Administration
FDA -	Food and Drug Administration
FEM -	Finite Element Methods
FFTW -	Fastest Fourier Transform in the West
FM -	Frequency Modulation
fMRI -	Functional Magnetic Resonance Imaging
FPGA -	Field Programmable Gate Array
GB -	Gigabyte
GLSL -	Graphic Language Shading Language
GPGPU -	General-Purpose Graphics Processing Unit
GPU -	Graphic Processing Unit
$h$ -	Planck's Constant
H -	Homography Matrix
$h$ -	Planck Constants ,
HIPAA -	Health Insurance Portability & Accountability Act
HLSL -	High Level Shader Language
HPC -	High Performance Computing
HSV -	Human Visual System
HU -	Hounsfield Units
$hv$ -	Energy Carried by Each Photon

I -	Intensity
IV -	Integral Videography
k -	Boltzmann constant
KB -	Kilobyte
kNN -	k-Nearest Neighbour Rule
$K_s$ -	Reflection Constant
$L_c$ -	Light Intensity Curve
LM -	Linear Memory
LMIP -	Local Maximum Intensity Projection
LoD -	Level-of-Details
LUT -	Look Up Table
MDFT -	Multidimensional Discrete Fourier Transform
MIP -	Maximum-Intensity Projection
MPR -	Multiplanar Reformation
MPU -	Multi-Level Partition of Unity
MRA -	Magnetic Resonance Angiography
MRF -	Markov Random Field
MRI -	Magnetic Resonance Images
MRT -	Magnetic Resonance Tomography
MS -	Multiple Sclerosis
$\mu$ -	Emission Coefficient
n -	Direction
$\check{N}$ -	Number of Photons
NL-means -	Non-Local Means Modes
NMRI -	Nuclear Magnetic Resonance Imaging
nvcc -	Nvidia CUDA Compiler
NVIDIA -	American Global Technology Company, California
$O_c$ -	Colour Curve of Object
OpenGL -	Open Graphic Language
PCA -	Principal Component Analysis



PET -	Positron Emission Tomography
Pixel -	Picture Element
PVE -	Partial Volume Estimation
$R(x,n,v)$ -	Radiance
RAM -	Random-Access Memory
$R_c$ -	Resulting Intensity Curve
Regs -	Register
RF -	Radio-Frequency
RGBA -	Red Green Blue Alpha
$s$ -	Distance
SIMD -	Single Instruction Multiple Data
SIMT -	Single Instruction, Multiple Thread
SMs -	Streaming multiprocessor
SPECT -	Single-Photon Emission Computed Tomography
SPs -	Streaming Processors
SVM -	Support Vector Machine
SVR -	Singular Value Decomposition
$s_x, s_y, s_z$ -	Scale Factors along x, y, z axes
T -	Temperature measured in Kelvin
T1-FLASH -	T1-Fast Low Angle Shot Magnetic Resonance
T1-MPRAGE -	T1-Magnetization Prepared Rapid Gradient Echo
TA -	Tensor Approximation
Tcl -	Tool Command Language
$T_s$ -	Transformation Matrix for Scaling
$U_i$ -	Points on Plane
$U_i'$ -	New sets of points on Plane
V -	Vanishing Point
$V(x,y,z)$ -	Discrete regular volume buffer
$V(x,y,z,d)$ -	Three dimensional data
VDVR -	Verifiable Direct Volume Rendering

VTK -	Visualization Toolkit
$W_a$ -	Weight of Ambient
$W_d$ -	Weight of Diffuse
WHO -	World Health Organization
$W_s$ -	Weight of Specular
X, Y, Z -	Coordinates Notation
XML -	Extensible Markup Language
Z -	Ground Plane
$\alpha_k$ -	Opacity
$\gamma$ -	Gyromagnetic Ratio of the nucleus in rad/T/s
$\delta E$ -	Radiant Energy interval $d\nu$ around $dt$
$\theta_k$ -	Transparency of the Material
$\nu$ -	Frequency through a in
$\chi$ -	Absorption Coefficient
$\psi(x,n,\nu)$ -	Photon Number Density

## CHAPTER 1

### INTRODUCTION

#### 1.1 Background Study

Throughout the history of humankind, visual imagery is seen as an appropriate way to communicate both abstract and concrete ideas to realization. Visualization is a way of making a form of mental vision, image or picture of something that is not visible, present to the sight or an abstraction, visible to the mind (The Oxford English Dictionary, 1989). Visual images are created through visualization, serving as models through which future things emerge. Some of the ancient uses of visualization are the European cave painting, the introduction of geometry by the ancient Greek and the description of locations in form of map.

Visualization spans through a wide spectrum of knowledge domain, however, it can be broadly categorized into scientific and information. Scientific visualization focuses on physical data such as meteorology, human body and earth while information visualization focuses on abstract, non-physical data such as financial data, bibliographic sources and statistical data (Teyseyre & Campo, 2009).

Volume Visualization is a domain within scientific visualization concerned with the representation, manipulation, modeling and rendering of volumetric datasets. Such volumetric datasets are represented as a 3-D discrete regular grid of volume elements (called voxels), stored in a discrete regular volume buffer  $V(x,y,z)$  (Kaufman, 1991). Medicine, Engineering, Geology and Pharmacology are among those fields that are massively benefiting from volumetric datasets. With the evolution of modern

technology, volume visualization has been extensively pushed into many applications, especially with arose consequence production of enormous data from medical community. Such creation of great amount of data has created more challenges and difficulties for the extraction of valuable information, analysis and its explanation in an intuitive way. Undoubtedly, CPU, as a functional processing device has high clock speed, facilitating its competencies for general-purpose tasks, but CPU has no parallel processing capabilities (Qin et al., 2012). Consequently, parallel computing is an alternative promising platform to accelerate visualization of medical volumetric datasets.

## 1.2 Brain Anatomy and Abnormalities

The relevance of brain in human being cannot be over-emphasized. Whereas, brain does not only exist in human being, it exists as well in other mammals. However, human brain is about three times larger, with around one hundred billion neurons (Kasthuri & Lichtman, 2010). Human brain is the center of nervous system controlling all activities of the human body, from self-control, reasoning, planning to vision, with all features greatly pronounced, enlarged and developed. Skull houses many brain slices. To perceive the complexity of the brain, each of the slices that made up the skull exists in certain measured thickness (ranges from 1 - 5mm) with each slice having distances in-between (ranges from 1 - 5mm) relative to image acquisition device employed.

Blood vessels, blood flows and the fluids surrounding the brain may contain different types of abnormalities. *Vascular abnormalities* may occur in the brain whenever abnormalities involve *arteries* or *veins*. In certain cases, there could be *blockages* in one of the blood vessels in the brain, depriving the brain of its functional flow of blood and oxygen. Vascular abnormalities are deadly medical cases that usually lead to *stroke*. Among other life-threatening abnormal conditions in the brain are *brain lesions*, as a result of abnormal tissue area in the brain, *brain tumor*, *hypertension*, *diabetes*, *walderstrom's macroglobulinemia* and *penetrating brain injury*.

Brain tumor is an abnormal growth of tissue in the brain. It may originate within the brain itself (primary tumor) or from other part of the body and travels to the brain

(secondary or metastatic tumor). While there are about two hundred and twenty (220) types of brain tumor classifications, brain tumor ranges from least aggressive, the benigns, which are non-cancerous, to the most aggressive, the malignants that are cancerous. However, most medical institutions use World Health Organization (WHO) standards for their classification. *Glioblastomas* is a malignant tumor that originates from the brain (primary tumor). Patients with *Glioblastomas* live an average of 12 - 14 months, although the medical communities hope for its medical long-term transfer into a more chronic disease for increase in life span of patients to 10-15 years. However, there is unlikely development of such cure within short expected time frame (Bredel, 2009). In the diagnosing procedures of most of these brain abnormalities, medical community has benefited immensely from the image modalities techniques such as MRI and CT.

Magnetic Resonance Images (MRI) sprung up in few decades ago and its significance is clearly noticed specifically in its ability to assign distinguishing intensity values to different levels of tissue densities. MRI is a non-invasive medical diagnostic technique for imaging human interior anatomical structures. MRI machine signal scans points-by-points into the patient's brain anatomical structures, creating a map, which it captures in *binary codes (1, 0)* and stored as 2-D datasets using mathematical function called *Fourier Transform*. MRI technique utilizes strong magnets and pulses of radio waves to manipulate the natural magnetic properties in the human body. Considering the fact that MRI does not use X-ray techniques unlike CT, there are no known biological risks involved when a patient is exposed to MRI scan. Moreover, it produces better images of organs, soft tissues and the interior structure of bones than those of other brain scanning technologies such as Computed Tomography (CT) and Positron Emission Tomography (PET).

The conventional MRI techniques include *axial*, *coronal* or *sagittal* orientation of *T1-weighted*, *T2-weighted* and *T\*2-weighted*. However, a number of specialized MR imagery is available for special purposes. *Magnetic Resonance Angiography (MRA)* is primarily designed for imaging *blood vessels* of the brain, to generate images of the *arteries* for *stenosis (abnormal narrowing)*, *occlusion* or *aneurysms*. *Diffusion Tensor Imaging (DTI)* is for determination of *magnitude and direction* of water; based on the principle of diffusion, the movement of water molecules from the region of higher

concentration to the region of lower concentration. The *T1-Fast Low Angle Shot Magnetic Resonance (T1-FLASH)* for *glioma tumor* and *lesions*, the *T1-Magnetization Prepared Rapid Gradient Echo (T1-MPRAGE)* which is for detecting *metastatic brain tumors*, are other specialized MR techniques employed in medical diagnosis.

### 1.3 Motivation

The physical world around us is in three-dimensional (3-D); yet traditional cameras and imaging sensors are only able to acquire and show two-dimensional (2-D) images that lack the depth information (Geng, 2011). The 2-D cross-sectional images produced from imaging techniques such as CT and MRI scanners are generally difficult to analyze. With this, the practice of surgical pathology involving the use of microscope to view tissue mounted on glass slides still persist significantly over many decades. In such usual cases of handling huge information embedded in each pixel of 2-D images, analyzing to deduce the position relationship between focus of infection and three dimensional geometry, estimating size and shape of focus of infection (Wu et al., 2010) usually require mental visualization of medical professionals based on their experience and expertise. This procedure is tedious, time-consuming and prone to error. Figure 1.1 and Figure 1.2 illustrate the conventional pathologist's procedure of analyzing scanned images of patients and the visualization-assisted procedures respectively.

Feature detection and local mapping of internal features are still open topics in the computer-aided diagnosis of biological disorders and pathologies. Although volume rendering has recorded good ability in depicting internal data features, however, locating object boundaries and revealing internal data features of interest are still challenging task due to the usual occlusion of features of interest by other volume structures (Kirmizibayrak et al., 2011; Gabor, Tornai & Cserey, 2010). Implicit visibility of tiny features, through allocation of transparency based on scalar values and assigning of transparency based on localized gradient magnitude for region of interest, are challenging issues. The difficulties of setting proper mapping functions to convert

original volumetric data to renderable color and opacity values limit the application of volume rendering (Guo, Mao & Yuan, 2011).

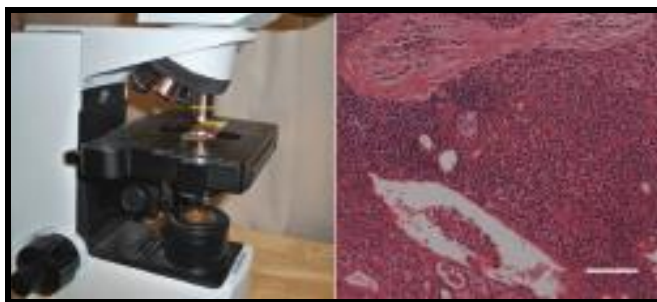


Figure 1.1: Conventional pathologists' slides viewing microscope (Jeong et al., 2010)



Figure 1.2: Clinical support with visualization

Medical visualization systems are developed to transform large and complex stacks of datasets into effective visual presentations for immediate medical diagnosis and therapy procedures. Volume rendering can be implemented to produce quality images, however, this technique still has a major outstanding drawback of “timely” generation of

such images (Yun & Xing, 2010). These medical scanners usually produce hundreds of 2-D slices requiring intense algorithm optimization. A computer-assisted brain diagnosis system that could effectively serve its purpose must be able to achieve not only fast generation of 3-D model of datasets but also the entire streams of datasets' processing within an interactive speed. The promise of computer-based surgical planning is to provide better surgical results with fewer procedures, decreased time in the operating room, lower risk to the patients (increased precision of technique, decreased infection risk), and lower resulting cost (Kumar & Rakesh, 2011).

Most of the previously developed medical visualization systems have shortcomings in:

1. reconstructing 2-D sequence of human organ, soft tissue and lesions sectional images to 3-D model, (Geng, 2011; Wu et al., 2010).
2. detecting, mapping and isolating abnormalities / tumor for surgery and/or disease diagnosis procedure, (Kirmizibayarak et al., 2011; Gabor, et al., 2010; Guo et al., 2011).
3. handling mass data within a considerable interactive speed, extensive application interoperability and at a low resulting cost (Yun & Xing, 2010; Kumar & Rakesh, 2011).

Thus, the main concentration of this study is to reconstruct sequence of 2-D imagery into 3-D model capable of clearly detecting, mapping and isolating abnormalities / tumor in MR imagery within a considerable interactive speed, extensive application interoperability and at a low resulting cost for optimum use in medical diagnosis and therapy treatment.



## 1.4 Research Questions

This study aims to solve the following research questions:

1. How to reconstruct 2-D sequence of brain MRI into 3-D model?
2. How to detect, map and isolate brain abnormalities / tumor for surgery and/or disease diagnosis procedures?
3. How to handle mass volume of volumetric brain MRI datasets within a considerable interactive speed, extensive application interoperability and at a low resulting cost?

## 1.5 Research Objectives

The objectives for this research are as follows:

1. To propose new approaches for brain volume visualization by introducing
  - a framework for reconstructing sequence of 2-D cross-sectional images to 3-D model,
  - a feature and edge detection scheme that can allocate transparency based on scalar values and assign transparency based on localized gradient magnitude for edge detection of region of interest in the data volume,
  - a technique with automatic local feature mapping scheme that can isolate abnormalities / tumor and reveal internal features of brain blood vessels,
  - algorithms within the framework that are robust enough to handle mass volumetric data within a considerable interactive speed, extensive application interoperability and at a lower resulting cost.
2. To design and implement a visualization system (*SurLens*) based on the proposed approaches.
3. To compare the volume visualization results of *SurLens* with existing approaches.

## 1.6 Scope of the Research

This research focuses on the design of *SurLens* framework and the implementation of *SurLens* volume visualization system. The study is limited to reconstructing and locating abnormalities / tumor in Magnetic Resonance (MR) Imagery of the brain in 3-D model. Focus is on obtaining quality 3-D images, sufficient enough to reveal detail internal information of datasets using the MRI datasets from the department of Surgery, University of North Carolina, Chapel Hill, United States. The study concentrates on Magnetic Resonance Angiography (MRA) datasets, however, Diffusion Tensor Imaging (DTI), T1-Fast Low Angle Shot Magnetic Resonance (T1-FLASH) and T1-Magnetization Prepared Rapid Gradient Echo (T1-MPRAGE) would also be considered. The development of the proposed visualization system would be within C# programming language environment, built on top of visualization toolkit (VTK) libraries and on parallel computing platform, Compute Unified Device Architecture (CUDA).

## 1.7 Organization of the thesis

To disseminate the findings of this research, concise investigation is presented into the field of visualization, human brain anatomy and its associated abnormalities.

In order to properly draw attention of the readers to some of the fundamentals of this research, Chapter 2 commences with general introduction of volume visualization and volumetric image datasets. Datasets pre-processing techniques and medical volume visualization as a whole is reviewed. Parallel processing procedures, specifically CUDA technology and previously proposed software components in this domain are extensively reviewed and presented. Strengths and weaknesses of previously proposed frameworks, schemes, algorithms and techniques are presented. The chapter describes and compares ten (10) recently proposed volume visualization frameworks in their entirety, in justification of the newly proposed framework, schemes, algorithms and techniques in this study.

Chapter 3 discusses the procedural research methodology, numerical computations and data structures used in the development of *SurLens* visualization system. The framework, schemes, algorithms, techniques and data collection for the development of *SurLens* visualization system are presented. Chapter 4 focuses on the designs and implementation of the proposed *SurLens* Visualization system for volumetric brain MRI datasets.

Evaluation results and discussion in comparison with two (2) notable, previously developed visualization systems are presented in Chapter 5 while Chapter 6 concludes the research, summarizes the major contributions of the study and presents the future works.

## CHAPTER 2

### VISUALIZATION OF VOLUMETRIC DATASETS

#### 2.1 Introduction

Visualization is a phenomenon existing in our day-to-day life. Over a thousand years ago, visualization has been used in the data plots, maps and scientific drawings. As far back as 1137 A.D, visualization was used to draw the map of China and the very famous map of Napoleon's invasion of Russia in 1812 (Owen, 1993). Visualization could be defined as a tool or method for interpreting image data, fed into a computer and for generating images from complex multi-dimensional data sets (McCormick, DeFanti & Brown, 1987). Informally, visualization engages the human vision and the processing power of human mind in the transformation of data or information into visual images referred to as pictures.

Visualization has received many descriptive terminologies over the years. Scientific visualization was first fundamentally used in 1987 (Rosenblum et al., 1994) and its seen as a representation of numerical data in a way that extrapolates meaningful information to understand or analyze interesting feature the data might hold. Data visualization is a more general term that implies treatment of data sources beyond the sciences and engineering. This encompasses marketing, business and financial data. More often, the term information visualization is becoming more pronounced. It is used to describe visualization of abstract information such as hypertext documents on the

World Wide Web, directory or file structures on a computer or abstract data structures (InfoVis, 1995).

Visualization is also seen as a method of extracting meaningful information from complex dataset through the use of interactive graphics and imaging (Kaufman, Cohen & Yagel, 1993), hence, computer graphics and image processing (or imaging) are tools for visualization. Computer graphics is the creation of images using computer, which encompasses 2-D paint techniques, drawing or rendering techniques. The output of computer graphics is an image. With image processing, we can define techniques to transform (rotate, scale, shear), extract, analyze and enhance images. Visualization focuses on exploring, transforming, viewing data as image in order to gain understanding and insight into the data. Computer graphics is used as a tool to produce the output for visualization. However, this study specifically tread the path of volume visualization, which is typically identified with the rendering, modeling, manipulation and representation of datasets (Kaufman, 1991; Kaufman, 1996).

Volume visualization is an important diagnostic tool in modern medicine. With computer imaging techniques such as Computed Tomography (CT) and Magnetic Resonance Imaging (MRI), internal information of a living patient is captured. The information is captured in form of slice-planes or cross-sectional images of patient which could be compared to the conventional photographic X-ray. A slice consists of a series of number values representing the attenuation of X-rays (in case of CT) or the relaxation of nuclear spin magnetization (MRI) (Krestel, 1990). However, with applied and sophisticated mathematical techniques, the slice-planes could be reconstructed and gathered into a volume of data.

Generally, with the slices, the series of number values are arranged in either a matrix pattern or regular array. However, with huge amount of information data in the slice, it is not possible to understand the data in its raw form, even with a trained eye. This is where the gray scale value comes in. Computer only understands 0's and 1's, whereas, human being cannot firmly relates the codes to meaningful information, possible solution is to represent the number values in 2-D cross-section that could be more useful with human vision system. Hence, such representation requires understanding the way medical imaging device scans.

This chapter reviews visualization of volumetric datasets and presents earlier frameworks from which medical volume visualization can be facilitated. After outlining broad collection of volumetric data acquisition methodologies, varying volume rendering techniques are described. The chapter extrapolates image reconstruction approaches, direct volume visualization techniques; possible optimization procedures specifically parallel processing approaches and their outstanding issues, which crystalize the research direction for this study. The weaknesses and strengths of each of the previous techniques are discussed. The strengths and weaknesses of ten (10) recently proposed volume visualization frameworks in entirety, including their proposed schemes, algorithms and techniques, are presented and compared in justification of the proposed framework, schemes, algorithms and technique in this study.

## **2.2 Volume Visualization**

Volume visualization is a sub-field of scientific visualization that extracts meaningful information from volumetric data using interactive graphics and imaging, and it is concerned with volume data representation, modeling, manipulation, and rendering (Suter et al., 2011). Volume visualization is an important tool for visualizing and analyzing data sets with its extensive application into such areas as biomedicine, computational fluid, finite element models, computational chemistry and geophysics. Magnetic Resonance (MR) Imagery and Computed Tomography (CT) are both imaging techniques benefiting optimally from volume visualization. Such numerical simulations and sampling devices create images of the human body for clinical diagnosis while volume visualization presents such datasets for viewing and clinical analyzing of the anatomical structures. Over recent years, volume visualization is continually evolving as visualization approaches, especially with the advent of faster processing devices. One of the challenges depriving the usage of volume visualization is the memory system to support volume processing (Suter et al., 2011; Ma, Murphy & O'Mathura, 2012).

Two-dimensional (2-D) data is represented as X and Y axes. These are mere flat structures in horizontal and vertical axes. Any image we have in this form, if turned to

its other sides, will become a line. Hence, a 2-D structure has corners or vertices and sides in two planes and cannot provide detail information embedded in image data. However, the 2-D representation can be re-represented in three-dimension (3-D), using mathematical models which has X and Y planes (just as 2-D image) but a Z-axis inclusive, this gives the image more features such as rotation. This third axis added faces to the 3-D structures, making the data available for real world simulation of the imaged object.

Since, there is a one-to-one correspondence between the pixel value in the image scan and a specific tissue of a patient, the numbers could be assigned a specific gray scale value. Displaying the data on the computer screen at this stage will emerge the structures in the patient's data. The emerged structures are as a result of the interaction of the human visual system with data spatial organization and the chosen gray-scale values. With this approach, its being possible to translate what computer represents as series of numbers into the corresponding cross-section of human body; the skin, the bone and the tissue. A more useful result could be made available for diagnosis by extending the 2-D into 3-D technique. In this case, the image slices are gathered as a volume of data. With 3-D technique, we can reveal the entire anatomical structure of a living patient without the intervention of surgery.

With the inability of the medical image scanners to present human anatomical structures in 3-D format, reconstruction procedure is the alternative. Reconstruction is a reverse engineering technique of 2-D MR imagery to 3-D. This is achieved in the medical diagnosis and disease management using the combination of computer graphics and image processing tools, the resulting 3-D data could serve as information for *opinion making and intervention planning* on a living patient without any prior mandatory surgical operation.

### **2.3 Volumetric Image Datasets**

The first step towards volume visualization is the acquisition of volumetric data. Typical set of data samples is represented as  $V(x,y,z,d)$ , in the case of a three- dimensional data,

with  $d$  representing the data property at a location determined by  $x, y, z$ . To describe value at any  $d$  continuous location, *zero-order (the Nearest Neighbor)*, *first-order (trilinear also called piecewise function)* and *higher-order interpolation* are possible options. The region of constant value that surrounds each sample in *zero-order interpolation* is known as a *volume cell* (commonly interchangeably referred to as *voxel (volume element)* or *grid location* or *sample points*) with each voxel being a rectangular cuboid having six faces, twelve edges and eight corners (Kaufman, 1996). Dataset is a collection of volume elements. However, there is variation in the spatial and intensity resolution of images produce by different medical imaging devices. This section presents some of the commonly used tools for volume data acquisition.

It is important to discuss the *topology* or *geometry* in which *volumetric data* must be. Data samples may exist as *scalar data*, holding such values as temperature, pressure and density, or exist as *vector* (e.g. velocity) or *tensor* (e.g. Finite Element Methods (FEM) modeling). Typically, a volume dataset  $V$  is a set of element (Winter, 2002) defined as:

$$V = \{ \nu_i(x, y, z) \mid i = 1, 2, \dots, n \}$$

$(x, y, z)$  is a point in 3-D space,  $\mathbb{E}^3$

$\nu_i(x, y, z)$  could be scalar, vector or tensor, which is defined as follows:

- a scalar function  $f : \mathbb{E}^3 \rightarrow \mathfrak{R}$ ;
- an n-dimensional vector function,  $f^n : \mathbb{E}^3 \rightarrow \mathfrak{R}^n$ , or
- a k-ranked tensor function,  $f^{n^k} : \mathbb{E}^3 \rightarrow \mathfrak{R}^{n^k}$ ,

*Scalar* and *vector* functions are representation of special cases of tensor functions with ranks 0 and 1 respectively. Usually in volume visualization, a total function is given by a physical or simulated object and then sampled at discrete points which is stored as discrete set of elements resulting in the formation of the defined dataset  $V$ . Figure 2.1 is the representation of volumetric data in Cartesian grid.



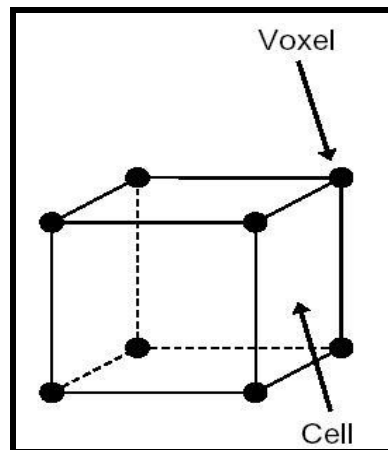


Figure 2.1: Volumetric Data in Cartesian Grid

Speray & Kennon (1990) categorized volume *dataset V* into *structured* and *unstructured* based on the topology of the *dataset*. In line with such categorization, the topology of structured data is well defined in each of its three orthogonal planes. This category includes cartesian, rectilinear and curvilinear grids. Unstructured grids are complex and difficult to use because their structures are not implicitly defined by data arrangements. However, *rectilinear grids* can be defined in *computational space* and classified as being *regular* or *irregular* in structure. If the spacing between samples along each axis is constant along the three orthogonal axes ( $x, y, z$ ), which is mostly the case, the *dataset V* is called *isotropic*. In certain cases, there might be separation along each axis in the dataset sample but different between the axes, the *dataset V* is referred to as *anisotropic*. Hence, if  $V$  is defined on a *regular grid*, a *3-D array* (commonly referred to as *volume buffer*, *3-D raster* or *cubic frame buffer*) is used to store the values and  $V$  is referred to as *array of values  $V(x, y, z)$*  defined only at grid locations. Figure 2.2 shows the different data structure grids.

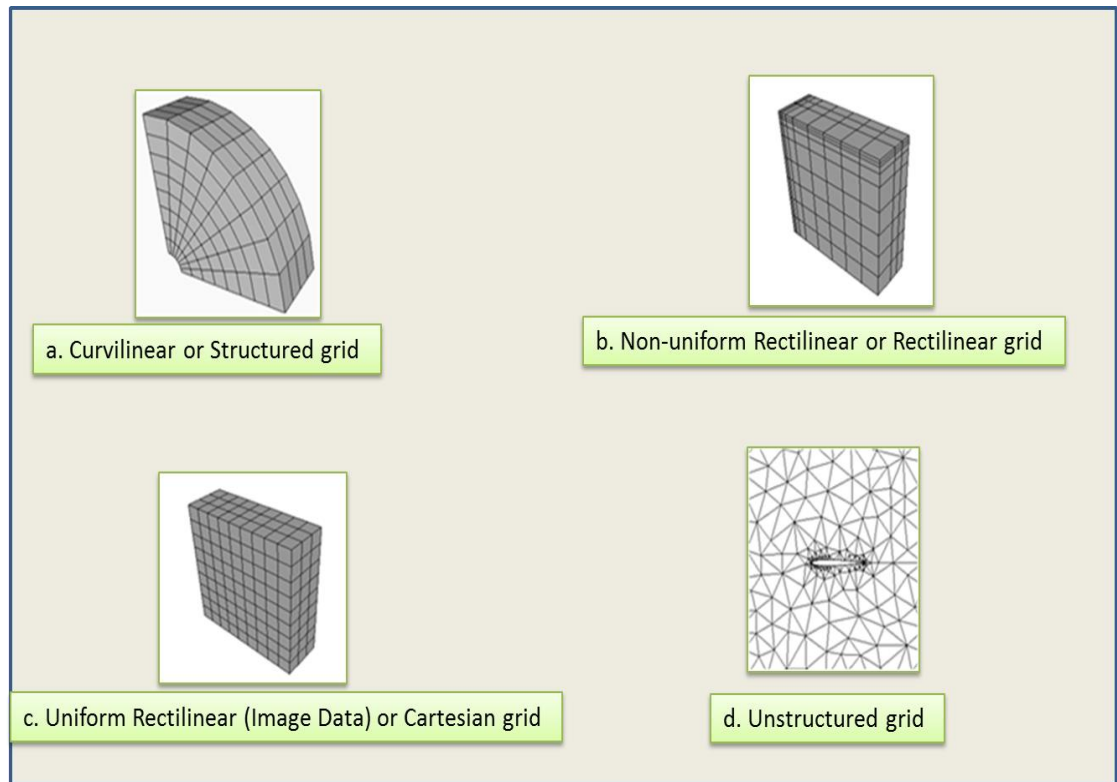


Figure 2.2: Data Structure Grids

## 2.4 Medical Imaging Modalities

Volume visualization became feasible with the revolution in image acquisition for extensive medical diagnosis and pre-treatment planning. The medical science that uses electromagnetic radiation, ultrasonography or radioactivity for evaluation of body tissues in case of injury or disease is referred to as *diagnoses medical imaging*. However, electromagnetic radiation can either be ionizing or non-ionizing. This section gives a brief overview and concepts of some of medical imaging modalities.

X-ray is the oldest imaging technique widely used throughout the world. It is an ionizing radiation technique discovered by the German physicist in 1895 by Wilhelm Conrad Röntgen (Yang, Guang-Zhong & Firmin, 2000). The discovery of Röntgen in that century drives the use of electromagnetic radiation in the form of ionizing radiation (gamma and X-rays) in an unprecedented speed for diagnostic radiology. The basic

principle for using X-ray involves passing of beam of X-rays, produced by an X-ray tube to selected parts of the body. There was an attempt to reconstruct images from projections as at 1940, this was even planned before the advent of modern computer technology. Gabriel Frank achieved this with the plan of describing the basic idea of modern tomography including such concepts as sonograms and optical back projection (Hsieh, 2002). About 16 years later, Allah M. Cormack furthered the research objectives with some experimental works based on reconstructive tomography.

$$\text{CT Number} = (\mu - \mu_{\text{water}} / \mu_{\text{water}} - \mu_{\text{air}}) \times 1000 \quad (1)$$

In 1967, the first CT scanner was developed by Godfrey N. Hounsfield in England at the Central Research Laboratory of EMI, Ltd (Hounsfield, 1973). Hounsfield investigation on pattern recognition techniques shows that if X-ray is passed through a body from different directions, this would result in its' internal body reconstruction. In his trials in 1969, test objects were scanned with isotope source that required a scan time of 9 days per image (Kalender, 2006).

Research usage of any of the image modalities depends on the intended image area to extract. Some could successfully extract certain information called “*Morphological Information*” while others are very useful in extracting “*physiological or functional information*”. *X-ray*, *CT* and *MRI* are typical examples of former while *PET* and *SPECT* are examples of the later. However, such specific features and functionalities justify their usage in medical community. Section 2.4.3 explains specific clinical relevancies of these image modalities.

### 2.4.1 Computed Tomography

Computed tomography (CT) is a widely adopted imaging modality with many clinical applications from *diagnosis* to *procedure planning* (Merck, 2009). Computed Tomography is a technique of X-ray photography in which a single plane of a patient is scanned from various angles in order to provide a cross-sectional image of the internal structure of that plane (Hsieh, 2002). Conventional radiography uses the relative

distribution of X-ray intensities for its measurement. It involves sending of uniform intensity X-ray through a patient from an X-ray source of intensity  $I_o$  and corresponding exiting of the X-ray with intensity  $I(x, y)$  from the other side, which then interact with a radiography film sheet. The different paths through the material will alternate the X-rays by varying amounts, based only on the mass attenuation coefficient ( $\mu$ ), since the *distance* ( $d$ ) is the same on all point of the radiography film (Shabaneh et al., 2004). CT uses attenuation as the judgments of its measurements as the X-ray is scanned through the patients.

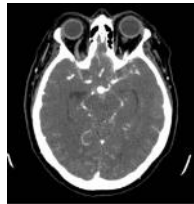


Figure 2.3: An example of a CT slice, a head scan (Lundström, 2007)

The patient is scanned using an X-ray source from one side of the plane and the detector placed on the opposite side is used to measure the attenuated X-ray, which is recorded by computer. After the first scan through the plane, the X-ray source and the detector rotate with a particular predefined amount for another translational scan. Hence, an X-ray technique involves passing electromagnetic radiation through the body. This is usually presented as CT Number, expressed in “*Hounsfield Units*” or “HU” named after Godfrey Hounsfield. A *positive CT* indicates a tissue is more attenuating than water while a *negative CT* denotes a tissue with lower density than water.

#### 2.4.2 Magnetic Resonance Imaging

Magnetic Resonance Imaging (MRI) technique has been one of the primary tools employed in medical diagnosis since the first publication of human body image in 1977 (Damadian, Goldsmith & Minkoff, 1977). MRI imaging technique is completely

different from that of Computed Tomography as it uses energy sources as its imaging procedure rather than ionizing radiation technique of X-ray. In the early years of existence of MRI, it was referred to as *Nuclear Magnetic Resonance Imaging (NMRI)* since it was developed from knowledge gained in the study of nuclear magnetic resonance (Amruta, Gole & Karunakar, 2010). The term NMRI is sometimes still in use when discussing non-medical devices of the same NMRI principle. However, in medical imaging, magnetic resonance tomography (MRT) may sometimes be interchangeably used for MRI. The procedure requires the usage of a strong magnetic field for spin alignment of hydrogen nuclei (photons) in the body.

The spin synchronizes as the radio-frequency (RF) pulse matches the nuclear resonance frequency of the photons. As the pulse is removed, different relaxation times are measured, that is, the times for the spins to go out-of-sync (Lundström, 2007). The density and chemical surroundings of the hydrogen atoms determine the measured value. Whilst some vectors will form alignment towards the direction of the main magnetic field, a slight majority will align themselves in the slightly lower energy state associated with the direction of the main magnetic field (Geoffrey et al., 2008). MRI creates its images as a result of the difference between two populations of vectors leading to the equilibrium net magnetic vectors. We could therefore say that, with MRI, a body is prepared for radio signal transmission on the FM bandwidth. The relative distribution of the vectors aligned within or against the main magnetic field is described by *Boltzmann distribution* as in equation (2).

The value of  $k$  is the *Boltzmann constant*,  $T$  is the *temperature* measured in *kelvin*,  $h$  is the *Planck constants*,  $\gamma$  is the *gyromagnetic ratio* of the nucleus in *rad/T/s* and  $B$  is the *strength of the magnetic field in tesla*,  $\hbar$  is a constant approximately equal to 3.14159. The number of spins in the lower energy level and the number of spins in the upper energy level are denoted by  $n_{\uparrow}$  and  $n_{\downarrow}$  respectively.

$$n_{\uparrow} / n_{\downarrow} = \exp(-\Delta E / kT), \text{ with } \Delta E = \hbar\gamma B / 2 \hbar \quad (2)$$

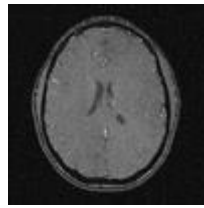


Figure 2.4: An example of an MRI slice, brain's Scan

### 2.4.3 Clinical Applications / Relevancies

MRI is the only chemically sensitive in-vivo imaging technique with high-resolution soft tissue contrast that allows physicians to peer deep inside the human body, producing clinically relevant images of soft tissue lesions and functional parameters of the body organs, without the use of invasive procedures or ionizing radiation such as X-rays (Cosmus & Parizh, 2011). However, with the knowledge gained in the course of this study, some of the clinical applications of CT and MRI, as being proven by researchers, solemnly depend on the required medical examination on the patient and in certain cases, the image modalities are seen to be complementary to each other in the diagnosis procedures.

With CT scan, herniated disc, spinal stenosis, fractures in the spine can be detected. It has also proven very useful in cartilage invasion and anatomy of the surrounding tissues. MRI has ability to demonstrate and characterize soft tissues hence useful in heart, muscles, brain, spinal cord, some head and neck tumors. Consequently, CT and MRI are mostly used image modality. In order to benefit optimally from CT and MRI, their combinatory techniques were introduced to create more impact features in medical imaging such as PET / CT and PET / MRI. Meanwhile, Magnetic Resonance Imaging (MRI) is the most recently applied technique, most commonly used in radiology to visualize the structure and functions of the body for many reasons among which is, it provides detailed images of the body in any plane with higher discrimination (Sun, Bhanu & Bhanu, 2009).

## 2.5 Dataset Pre-Processing Techniques

Pre-processing stage in volume visualization is to enhance the visual appearances of the images and the manipulation of the datasets' structures, to convert them from their acquired representation to spatial representation required and appropriate for visualization. However, a lot of caution needs to be exercised with image enhancements' procedures as poorly embarked approach may introduce image artefacts or even lead to loss of information in the datasets.

Segmentation, a key step and a large research area in visualization, is usually performed at the pre-processing step of volume visualization. As a matter of fact, different organs or tissues of an acquired volumetric data might have the same density or intensity hence segmentation stage and not only classification becomes essential. The fundamental principle guiding volume visualization is based on the fact that empowering the user to see a certain structure, using only classification is not always possible (Meißner et al., 2000). Though acquisition methods usually demand different level or extent of required segmentation but most methods require semi-automatic approach which invariably increases the overall processing time of datasets in volume visualization. Studies have shown that segmentation of brain MR is a compulsory, difficult and time consuming stage for volume visualization because of variable imaging parameters, overlapping intensities, noise, partial voluming, gradients, motion, echoes, blurred edges, normal anatomical variations and susceptibility artefacts (Lladó et al., 2012; Sha & Sutton, 2001).

This section reviews previous datasets pre-processing techniques and highlights the significant contribution of *SurLens* Dataset Pre-processing approach.

### 2.5.1 Filtering, Enhancement, Detection & Extraction

One of the key processes in the pre-processing is the removal of noise from MRI data. Some of the techniques used for MRI de-noising include non-linear filtering methods (Muhammed et al., 2011; Gupta, Anand & Tyagi, 2012) spectral subtraction (Liu et al.,

2012), wavelet-based thresholding (Agrawal & Sahu, 2012), anisotropic non-linear diffusion filtering (Zhang & Ma, 2010; Perona & Malik, 1990), Markov Random Field (MRF) models (An & An, 1984), wavelet models (Nowak, 1990), non-local means modes (NL-means) (Buades, Coll & Morel, 2005), and analytical correction schemes (Sijbers, 1998). Despite the fact that there are quite a substantial number of state-of-the-art methods for de-noising, accurate removal of noise from MRI is still a challenge; as all these methods are almost the same in terms of computation cost, de-noising, quality of de-noising and boundary preserving, which has retained MRI de-noising as an open issue that needs better improved methods (Bandhyopadhyay & Paul, 2012). Hence, de-noising methods at this current state of research are not reliable enough to fully support pre-processing stage of volume visualization. The main challenge in de-noising MRI is to preserve the edges and the details, at the same time to reduce noise in uniform regions (Diaz et al., 2011).

Edge detection or extraction is an important step in MRI data pre-processing. There are three steps in edge detection process (Senthilkumarn & Rajesh, 2008), the image filtering, the image enhancement, and the image detection. Image filtering is required in pre-processing because the target MRI images might have been corrupted through a number of circumstances like impulse noise, Gaussian noise, being common situations. More filtering procedures to reduce noise may results in loss of the strength of the edges (Senthilkumarn & Rajesh, 2009). Image enhancement emphasizes pixels where there is a significance change in local intensity values and is usually performed by computing gradient magnitude (Wen, Zhang & Jiang, 2008) while image detection usually based on thresholding criterion (Paulinas & Usinskas, 2007).

Quite a number of operators are usually used for image filtering, enhancement, and detection such as Sobel, Prewitt, Roberts, Laplacian of Gaussian, Zero-cross and cunny (usually refers to as Gaussian) operators. Among these set of techniques, Sobel operators' produces best sharpness and clear edges (Ponraj et al., 2011). Though Sobel operator has been proven to produce superior qualities compared to other techniques, it has also been confirmed inaccurate and sensitive to noise (VenuGopal & Naik, 2011). Therefore, since image filtering, enhancement, detection and extraction technique play a key role in the development of a reliable medical visualization framework, a better and a



contributing approach must be considered during the pre-processing stage of a volume visualization framework in order to improve accuracy and noise sensitivity interference.

As one of our contributions to this field, we have therefore designed and implemented a new algorithm for image filtering, enhancements, detection and extraction, actualized at the graphic execution phase of our framework, which is the main entry point of datasets into volume visualization. This is an improved and better approach tackling accuracies of image filtering, enhancements, detection and extraction by enabling the datasets to be processed at the main entry point of volume visualization in order to avoid any unwanted noise sensitivity. We do not observe any shortcoming of this design hence it is noted as an improvement over all the previously pre-processing approaches.

### **2.5.2 Volume Segmentation**

Brain MRI segmentation has been attracting attention for a while considering its significance in the medical image analysis and diagnosis. As each of the points in the image scan corresponds to a particular point in the human body structure, during segmentation process, each point in the scanned image and its correspondence to the tissue or organ is identified. A number of segmentation algorithms have been proposed in the past. Clustering-based (Kannan & Pandiyarajan, 2009), region-growing (Welinski & Fabijanska, 2011; Deng et al., 2010), active contour-based (Tanoori et al., 2011), watershed-based (Freitas et al., 2011) and morphological-based segmentation (Li et al., 2011) have been previously applied to brain MRI volume segmentation. Sethian (1999), Ben-Zadok, Riklin-Raviv & Kiryati (2009) and Cremers et al., (2007) have made appreciable contribution in the boundary-based segmentation procedures.

One of the notable studies in this regard is that of Bezdek, Hall & Clarke (1993). Bezdek et al. (1993) made a thorough review on MRI segmentation using pattern recognition techniques. The study categorized brain MRI segmentation algorithms into supervised methods and unsupervised strategies. Supervised segmentation strategy is based on some prior information or knowledge to perform segmentation while

unsupervised strategy performs brain MRI segmentation with no prior knowledge or information. The supervised methods are listed to include Bayes classifiers with labeled maximum likelihood estimators, the k-nearest neighbour rule (kNN) and artificial neural networks (ANN) while the unsupervised methods include Bayes classifiers with unlabelled maximum likelihood estimators or the fuzzy C-means (FCM) algorithms.

Though segmentation is usually performed at the pre-processing stage of volume visualization, being a key and a large research area, some studies separated the usual pre-processing stages distinctly from segmentation. Clarke et al. (1995) reviewed both pre-processing and segmentation methods of soft brain tissue. In the same vein, Styner et al. (2008) reviewed semi-automated and automated multiple sclerosis (MS) lesion segmentation approaches, analyzing MS lesions, pre-processing steps and segmentation approaches. More recently, Lladó et al. (2012) presented a review of brain MRI with the goal of helping diagnosis and follow-up of multiple sclerosis lesions in brain MRI.

In order to enhance the visual appearance of the brain MRI images, any possible artefacts will need to be removed. Removal of the contained artefacts could be done at this stage, done partly or delayed until the final entry point of the dataset into volume visualization phase, this depends on the design of the volume visualization framework. Whichever of the approach being adopted in the framework design, there must be adequate provision set aside in case of unexpected introduction of certain level of artefacts during the pre-processing phase.

Skull stripping is another important pre-processing step since fat, skull, skin and other non-brain tissues may cause mis-classifications in some approaches due to the intensity similarities with brain structures (Detta & Narayana, 2011). Some of the components of the brain require a particular MRI technique for their diagnosis, hence, without thorough skull stripping it might be difficult to have the intended structures' of study visible with volume visualization algorithms.

In cases where studies need to be carried out on more than one components structure of the brain e.g. tissue and fat, alignment of the soft brain images would be required. Aligning all the images from different modalities or MR images is known as registration (Zitova & Flusser, 2003). The precise steps involve include feature

## REFERENCES

- Agrawal, S. & Sahu, R. (2012). Wavelet Based MRI Image Denoising Using Thresholding Techniques. *International Journal of Science, Engineering and Technology Research (IJSETR)*. Vol. 1, Issue 3, September.
- Ahrens, J., Geveci, B., & Law, C. (2005). *The Visualization Handbook, ParaView: An End-User Tool for Large Data Visualization*. Burlington, MA: Elsevier, 717.
- Alim, U.R. & Möller, T. (2009). A Fast Fourier Transform with Rectangular Output on the BCC and FCC Lattices. *Proc. Eighth Int'l Conf. Sampling Theory and Applications (SampTA)*.
- Aliroteh, M. & McInerney, T. (2007). SketchSurfaces: Sketch Line Initialized Deformable Surfaces for Efficient and Controllable Interactive 3D Medical Image Segmentation, *Third International Symposium on Visual Computing (ISVC)*, LNCS 4841, Lack Tahoe, Nevada/California, November 26-28, pp. 542-553.
- Amruta, A., Gole, A. & Karunakar, Y. (2010). A Systematic Algorithm for 3-D Reconstruction of MRI based Brain Tumors using Morphological Operations and Bicubic Interpolation. *2<sup>nd</sup> International Conference on Computer Technology and Development (KCTD)*.
- An, S. & An, D. (1984). Stochastic Relaxation, Gibbs Distributions, and the Bayesian Restoration of Images. *IEEE Trans Pattern Anal Mach Intell* 6: 721-741.
- Archirapatkave, V., Sumilo, H., See, S.C.W. & Achalakul, T. (2011). GPGPU Acceleration Algorithm for Medical Image Reconstruction: *Ninth IEEE International Symposium on Parallel and Distributed Processing with Applications IEEE*.

- Baek, S.Y., Sheafor, D.H., Keogan, M.T., DeLong, D.M. & Nelson, R.C. (2001). Two-dimensional multiplanar and three-dimensional volume-rendered vascular CT in pancreatic carcinoma: interobserver agreement and comparison with standard helical techniques. *Am J Roentgenol* 176(6):1467–1473.
- Bandhyopadhyay, S.K. & Paul, T.U. (2012). Segmentation of Brain MRI Image A Review. *International Journal of Advanced Research in Computer Science and Software Engineering*. Volume 2, Issue 3, March 2012 ISSN: 2277 128X.
- Bentoumi, H., Gautron, P. & Bouatouch, K. (2010). GPU-Based Volume Rendering for Medical Imagery. *International Journal of Electrical, Computer, and Systems Engineering* 4:1.
- Ben-Zadok, N., Riklin-Raviv, T. & Kiryati, N. (2009). Interactive level set segmentation for image-guided therapy. In *IEEE Int. Symp. On Biomedical Imaging*, pages 1079–1082.
- Benzinga News. November 29, 2010. Kitware Offers Free Global Access to VolView at RSNA.
- Bezdek, J.C., Hall, L.O. & Clarke, L.P. (1993). Review of MR Image Segmentation Techniques using Pattern Recognition, *Med. Phys.* 20 (4) 1033–1048.
- Birk, M., Guth, A., Zapf, M., Balzer, M., Ruitter, N., Hübner, M. & Becker, J. (2011). Acceleration of Image Reconstruction in 3D Ultrasound Computer Tomography: An Evaluation of CPU, GPU AND FPGA Computing. *IEEE Conference on Design and Architectures for Signal and Image Processing (DASIP)*. On page(s): 1 – 8, E-ISBN : 978-1-4577-0619-6, Print ISBN: 978-1- 4577-0620-2.
- Bredel, M. (2009). Gene Connections Key to Brain Tumor. *Journal of the American Medical Association*. The U.S. National Cancer Institute, Cancer Newsletter. July, 20.
- Bremer, P.T., Weber, G.H., Tierny, J., Pascucci, V., Day, M.S. & Bell, J.B. (2011). Interactive Exploration and Analysis of Large-Scale Simulations Using

- Topology-Based Data Segmentation. *IEEE Transactions on Visualization And Computer Graphics*, Vol. 17, No. 9, pp. 1307- 1324.
- Buades, A., Coll, B. & Morel, J. (2005). A Non-Local Algorithm for Image Denoising. *IEEE Computer Society Conference on Computer Vision and Pattern Recognition*, pp 60–65.
- Bullitt, E., Zeng, D., Mortamet, B., Ghosh, A., Aylward, S.R., Lin, W., Marks, B.L. & Smith, K. (2010). The Effects of Healthy Aging on Intracerebral Blood Vessels Visualized by Magnetic Resonance Angiography: *Neurobiol Aging* 31(2): 290–300.
- Busking, S. Vilanova, A. & Wijk, J.V. (2007). Particle-Based Non-Photorealistic Volume Visualization,” *Visual Computer*, vol. 24, No. 5, pp. 335-346, May 2007.
- Cao, Y., Wu, G. & Wang, H. (2011). A Smart Compression Scheme for GPU-Accelerated Volume Rendering of Time-Varying Data. *IEEE International Conference on Virtual Reality and Visualization*, Page(s): 205 – 210.
- Carlos, D.C. & Ma, kwan-Liu (2009). The occlusion spectrum for volume classification and visualization, *IEEE Transactions on Visualization and Computer Graphics*, Vol. 15, No. 6.
- Chen, C. & Yang, J. (2011). Essence of Two-dimensional Principal Component Analysis and Its Generalization: Multi-dimensional PCA. *Second International Conference on Innovations in Bio-inspired Computing and Applications*.IEEE Computer Society.
- Chen, M., Kaufman, A. & Yagel, R. (2000). *Volume Graphics*, Springer (Eds.). London.
- Chen, Ming-Da., Hsieh, Tung-Ju. & Chang, Yang-Lang. (2011). Volume Data Numerical Integration and Differentiation Using CUDA. *IEEE 17th International Conference on Parallel and Distributed Systems*.
- Cheung, M.R. & Krishnan, K. (2012). Using Manual Prostate Contours to Enhance Deformable Registration of Endorectal MRI. *Computer Methods and Programs in Biomedicine* 108, 330-337.

- Chiueh, T.-C., Yang, C.-K., He, T., Pfister, H. & Kaufman, A.E. (1997). Integrated Volume Compression and Visualization. In Proc. IEEE Visualization, Pages 329–336. Computer Society Press.
- Chiw, C., Kindlmann, G., Reppy, J., Samuels, L. & Seltzer, N. (2012). Diderot: A Parallel DSL for Image Analysis and Visualization. Proceedings of the 33rd ACM SIGPLAN conference on Programming Language Design and Implementation. ACM New York, NY, USA, pp 111-120.
- Chu, H., Chen, L. & Yong, J. (2010). Feature variation curve guided transfer function design for 3D medical image visualization, 3rd International Conference on Biomedical Engineering and Informatics.
- Clarke, L.P., Velthuizen, R.P., Camacho, M.A., Heine, J.J., Vaidyanathan, M., Hall, L.O., Thatcher, R.W. & Silbiger, M.L. (1995). MRI Segmentation: Methods and Applications, *Magn. Reson. Imag.* 13 (3) 343–368.
- Cosmus, C. C & Parizh, M. (2011). Advances in Whole-body MRI Magnets. *IEEE transactions on applied semiconductor*, Vol. 21, No. 3.
- Courchesne, E., Chisum, H.J., Townsend J, Cowles, A., Covington, J., Egaas, B., Harwood, M., Hinds, S. & Gary, A. (2000). Normal Brain Development and Aging: Quantitative Analysis at in vivo MR Imaging in Healthy Volunteers. *Journal of Radiology*. Press GA. 216:672–682. [PubMed: 10966694].
- Cox, G., Maximo, A., Bentes, C. & Farias, R. (2009). Irregular grid Raycasting implementation on the cell broadband engine, 21st International Symposium on Computer Architecture and High Performance Computing.
- Creasey, H. (2003). Rapoport SI. The aging human brain. *Annals of Neurology*. 17:2–10. [PubMed:3885841].
- Cremers, D., Fluck, O., Rousson, M. et al. (2007). A probabilistic level set formulation for interactive organ segmentation. *Medical Imaging 2007: Image Processing*, 6512(1):120–129.

- Csébfalvi, B. & Domonkos, B. (2009). Frequency-Domain Upsampling on a Body-Centered Cubic Lattice for Efficient and High-Quality Volume Rendering. Conference on Vision Modeling and Visualization – VMV, pp. 225-232.
- Csébfalvi, B. & Szirmay-Kalos, L. (2003). Monte Carlo Volume Rendering. Proc. of IEEE Visualization, pp.449- 456, 2003.
- Da Silva, L.S., & Scharcanski, J. (2005). A lossless Compression Approach for Mammographic Digital Images Based on the Delaunay Triangulation. IEEE International Conference on Image Processing, ICIP. pp.11 - 758-61.
- Damadian, R., Goldsmith, M. & Minkoff, L. (1977). NMR in cancer: XVI. Fonar image of the live human body”, *Physiological Chemistry and Physics*, Vol. 9, pp. 97-100.
- Datta, S. & Narayana, P.A. (2011). Automated Brain Extraction from T2- Weighted Magnetic Resonance Images, *J. Magn.Reson.* 33 (4) 822– 829.
- Deng, W., Xiao, W., Deng, E. & Liu, J. (2010). MRI Brain Tumor Segmentation With Region Growing Method Based On The Gradients and Variances Along And Inside Of The Boundary Curve. 3rd International Conference on Biomedical Engineering and Informatics (BMEI).
- Diaz, I., Boulanger, P., Greiner, R. & Murtha, A. (2011). A Critical Review of the Effect of De-noising Algorithms on MRI Brain Tumor Segmentation. 33<sup>rd</sup> Annual International Conference of the IEEE EMBS, Boston, Massachusetts, USA.
- Dorgham, O.M., Laycock, S.D. & Fisher, M.H. (2012). GPU Accelerated Generation of Digitally Reconstructed Radiographs for 2-D/3-D Image Registration. *IEEE Transactions on Biomedical Engineering*, Vol. 59, No. 9. Pp. 2594 – 2603.
- Drebin, R., Carpenter, L., Hanrahan, P. (1988). Volume rendering, *Proceedings SIGGRAPH88*, pp 65–74.
- Fang, J., Varbanescu, A.L. & Sips, H. (2011). A Comprehensive Performance Comparison of CUDA and OpenCL. *IEEE International Conference on Parallel Processing*.

- Ferre, M., Cobos, S., Aracil, R. & Sánchez Urán, M.A. (2007). 3D Image Visualization and Its Performance in Teleoperation, HCI. International Conference, Peking, China. Virtual Reality, Vol.14, LNCS 4563, R. Shumaker (Hrg.); Springer, Volume 14, LNCS 4563, pp 669-707.
- Freitas, P., Rittner, L., Appenzeller, S. & Lotufo, R. (2011). Watershed-based Segmentation of the Midsagittal Section of the Corpus Callosum in Diffusion MRI. 24th Conference on Graphics, Patterns and Images 2011 24th SIBGRAPI Conference on Graphics, Patterns and Images. Pg 274-280.
- Friego, M. & Johnson, S. (2005). The Design and Implementation of FFTW3. Proc. of the IEEE, 93(2): 216-231.
- Gabor J. Tornai, G.J. & Cserey, G. (2010). 2D and 3D Level-Set Algorithms on CPU. 12th International Workshop on Cellular Nanoscale Network and their Applicatins (CNNA).
- Geng, J. (2011). Structured-light 3D surface imaging: a tutorial. Advances in Optics and Photonics 3, 128-160.
- Geoffrey S.P., Elizabeth, Charles-Edwards & Christopher, P. (2008). Applications of Computed Tomography, Magnetic Resonance Imaging and Magnetic Resonance Spectroscopy for Planning External Beam Radiotherapy, Current Medical Imaging Reviews, 4, 236-249.
- Ghorpade, J., Parande, J., Kulkarni, M. & Bawaskar, A. (2012). Gpgpu Processing in Cuda Architecture. Advanced Computing: An International Journal (ACIJ ), Vol.3, No.1.
- Gong, F. & Zhao, X. (2010). Three-Dimensional Reconstruction of Medical Image Based on Improved Marching Cubes Algorithm. International Conference on Machine Vision and Human-machine Interface.
- GPU Computing and the CUDA architecture (2009). NVIDIA CUDA Architecture Introduction & Overview, Version 1.1.
- Gu, S., Wilson, D., Wang, Z., Bigbee, W.L., Siegfried, J., Gur, D. & Pu, J. (2012). Identification of Pulmonary Fissures using A Piecewise Plane Fitting



- Algorithm. *Computerized Medical Imaging and Graphics*. *Computerized Medical Imaging and Graphics* 36 560– 571.
- Guo, H., Mao, N. & Yuan, X. (2011). WYSIWYG (What You See is What You Get) Volume Visualization. *IEEE Transactions on Visualization and Computer Graphics*, Vol. 17, NO. 12, on page(s): 2106 – 2114, ISSN : 1077-2626.
- Guo, H., Xiao, H. & Yuan, X. (2012). Scalable Multivariate Volume Visualization and Analysis Based on Dimension Projection and Parallel Coordinates. *IEEE Transactions on Visualization and Computer Graphics*, Vol. 18, No. 9, pp 119-120.
- Guo, H., Xiao, H. & Yuan, X. (2011). Multi-Dimensional Transfer Function Design Based on Flexible Dimension Projection Embedded in Parallel Coordinates. *Proc. IEEE Pacific Visualization Symp.*, pp. 19-26.
- Gupta, D., Anand, R.S., & Tyagi, B. (2012). Enhancement of Medical Ultrasound Images using Non-Linear Filtering Based on Rational-Dilation Wavelet Transform. *Proceedings of the World Congress on Engineering and Computer Science (WCECS)*. Vol. I October 24-26. San Francisco, USA
- Hadwiger, M., Kniss, J., Rezk-Salama, C., Weiskopf, D. & Engel, K. (2006). *Real-time volume graphics*, A K Peters Publications.
- He, X. (2009). Reconstruction of 3d microstructure of the rock sample Basing on the CT images. *Proceedings of the International Conference on Wavelet Analysis and Pattern Recognition*, Baoding, 12-15 July.
- Hege, H.C., Höllerer, T. & Stalling, D. (1996). *Volume Rendering - Mathematical Models and Algorithmic Aspects*. W. Nagel (Hrsg.) *Partielle Differentialgleichungen, Numerik und Anwendungen*. Konferenzen des Forschungszentrums Jülich GmbH, S. 227-255.
- Herlambang, N., Liao, H., Matsumiya, K., Masamune, K. & Takeyoshi, D. (2008). Real Time Autostereoscopic Visualization of Registration Generated 4D MR Image of Beating Heart, *Medical Imaging and Augmented Reality (MIAR)*, 4th International Workshop Tokyo, Japan, August 1-2, pp 349-358.

- Hernell, F., Ljung, F. & Ynnerman, A. (2010). Local ambient occlusion in direct volume rendering, *IEEE Transactions on Visualization and Computer Graphics*, Vol. 16, No. 4.
- Hong, L. & Shuhuil, M. (2010). High Precision Hybrid Technique of Surface and Volume Rendering. *Second International Conference on Computational Intelligence and Natural Computing (CINC)*.
- Hossain, Z., Alim, U.R. & Möller, T. (2011). Toward High-Quality Gradient Estimation on Regular Lattices. *IEEE Transactions on Visualization and Computer Graphics*, Vol. 17, No. 4, pp. 426 – 439.
- Hounsfield G.N. (1973). Computerized transverse axial scanning tomography, Description of system *Br. J. Radiol.*, 46 1016.
- Hsieh, J. (2002). *Computed Tomography Principles, Design, Artifacts, and recent Advances*, Spie Press.
- Hu, S. & Hou, W. (2011). Denosing 3D Ultrasound images by Non-local Means Accelerated by GPU. *IEEE International Conference on Intelligent Computation and Bio-Medical Instrumentation*, pp. 43-45.
- Jeong, Won-Ki., Schneider, J., Turney, S.G., Faulkner-Jones, B.E., Meyer, D., Westermann, R., Reid, R.C., Lichtman, J. & Pfister, H. (2010). Interactive Histology of Large-Scale Biomedical Image Stacks. *IEEE Transactions on Visualization and Computer Graphics*, Vol. 16, no. 6, November/December.
- Jinzhu, Y., Fangfang, H., Chaolu, F., Dazhe, Z. & Yanfei, W. (2011). An Accelerative Method for Multimodality Medical Image Registration Based on CUDA. *4th International Congress on Image and Signal Processing (CISP)*, pp. 1817 – 1821.
- Joemai, R.M.S., Geleijns, J., Veldkamp, W.J.H., De Roos, A. & Kroft, L.J.M. (2008). Automated cardiac phase selection with 64-MDCT coronary angiography, *AJR Am J Roentgenol* 191:1690–1697.
- Jovanovic, R. & Lorentz, R.A. (2012). A Combined Image Approach to Compression of Volumetric Data using Delaunay Tetrahedralization. *Conference on Image Processing (IPR), IET*. Pp. 1-6.

- Kainz, B., Portugaller, R.H, Seider, D., Moche, M., Stiegler, P. & Schmalstieg, D. (2011). Volume visualization in the clinical practice. *Augmented Environments for Computer Assisted Interventions (AE-CAI'11)*.
- Kalender, W.A. (2006). Review: X-ray Computed Tomography, *Institute of Physics Publishing Phys. Med. Biol.* 51, R29–R43.
- Kannan, S.R. & Pandiyarajan, R. (2009). Effective fuzzy c-mean Clustering technique for segmentation of T1-T2 brain MRI. *IEEE International Conference on Advances in Recent Technologies in Communication and Computing*. Pg. 537-539.
- Kasiri, K., Dehghani, M.J., Kazemi, K., Helfroush, M.S. & Kafshgari, S. (2010). Comparison Evaluation of Three Brain MRI Segmentation Methods in Software Tools. *IEEE Proceedings of the 17th Iranian Conference of Biomedical Engineering (ICBME)*.
- Kasthuri, N. & Lichtman, J.W. (2010). Neurocartography, *Neuropsychopharmacology*, 35, 342–343; doi:10.1038/npp.2009.138.
- Kaufman, A. (1991). *Volume Visualization (Tutorial)*. IEEE Computer Society Press, Los Alamitos, California.
- Kaufman, A. & Mueller, K. (2005). Overview of Volume Rendering, *The Visualization Handbook*, eds. C. Johnson and C. Hansen, Academic Press.
- Kaufman, A.E. (1996). Volume Visualization. *ACM Computing Survey*, 28(1): 165-167.
- Kaufman, A.E. (2000). Volume visualization: Principles and advances. *International Spring School on Visualization*, Bonn.
- Kim, J. & Jaja, J. (2009). Streaming Model Based Volume Ray Casting Implementation for Cell Broadband Engine, *Scientific Programming*, Vol. 17, no. 1-2, pp. 173-184.
- Kirk, D. & Hwu, W.-M. (2010). *Programming Massively Parallel Processors: A Hands-on Approach*. Morgan Kaufmann, 2010.
- Kirk, D.B. & Hwu, W.M.W. (2010). *Programming Massively Parallel Processors: A Hands on Approach*. New York: Elsevier, 2010.

- Kirmizibayrak, C., Radeva, N., Mike Wakid, M., Philbeck, J., John Sibert, J. & Hahn, J. (2011). Evaluation of Gesture Based Interfaces for Medical Volume Visualization Tasks. Proceedings of the 10th International Conference on Virtual Reality Continuum and Its Applications in Industry Pg. 69-74. ACM New York, NY, USA.
- Kitware News. October 10, 2002. Kitware Announces ParaView 0.6.
- Koo, J.J., Evans, A.C. & Gross, W.J. (2009). 3-D Brain MRI tissue classification on FPGAs, IEEE Transactions on image processing, vol.18, No.12.
- Krechetova, K., Glaz, A. & Platkajis, A. (2008). 3D Medical Image Visualization and Volume Estimation of Pathology Zones, NBC – 14<sup>th</sup> Nordic-Baltic Conference on Biomedical Engineering and Medical Physics, Latvia (IFMBE Proceedings) Vol. 20, pp 532-535.
- Krestel, E. (1990). Imaging Systems for Medical Diagnosis. Siemens, Aktienges, Munich. Krömer, P., Platoš, J. & Snásel, V. (2011). Differential Evolution for the Linear Ordering Problem Implemented on CUDA. IEEE Publications.
- Kumar, N., Nasser, M., Sarker, S.C. (2011). A New Singular Value Decomposition Based Robust Graphical Clustering Technique and Its Application in Climatic Data. Journal of Geography and Geology Vol. 3, No. 1.
- Kumar, T.S. & Rakesh, P.B. (2011). 3D Reconstruction of Facial Structures from 2D images for cosmetic surgery. International Conference on Recent Trends in Information Technology, ICRTIT MIT, Anna University, Chennai.
- Lai, Po-Lun & Yilmaz, A. (2008). Projective reconstruction of building shape from silhouette Images acquired from uncalibrated cameras. The International Archives of the Photogrammetry, Remote Sensing and Spatial Information Sciences. Vol. XXXVII. Part B3b. Beijing.

- Law, C.C., Henderson, A. & Ahrens, J. (2001). An Application Architecture for Large Data Visualization: A Case Study. *IEEE Symposium on Parallel and Large-Data Visualization and Graphics*. Pp. 125 – 159.
- Lei, G., Dou, Y., Wan, W., Xia, F., Li, R., Ma, M. & Zou, D. (2012). CPU-GPU hybrid accelerating the Zuker algorithm for RNA Secondary Structure Prediction Applications. *BMC Genomics*, 13 (Suppl 1):S14.
- Li, M., Zheng, X., Wan, X., Luo, H., Zhang, S. & Tan, L. (2011). Segmentation of brain tissue based on connected component labeling and mathematic morphology. *4th International Conference on Biomedical Engineering and Informatics (BMEI)*. pg 482-485.
- Lindholm, E., Nickolls, J., Oberman, S. & Montrym, J. (2008). NVIDIA Tesla: A Unified Graphics and Computing Architecture. *IEEE Micro*, 28(2):39–55.
- Lindholm, S., Ljung, P., Lundstrom, C., Persson, A. & Ynnerman, A. (2010). Spatial conditioning of transfer functions using local material distributions, *IEEE Transactions on Visualization and Computer Graphics*, Vol. 16, No. 6.
- Ling, F., Yang, L. & Wang, Zhong-Ke (2009). Improvement on Direct Volume Rendering, *Image and Signal Processing, CISP*.
- Ling, T. & Zhi-Yu, Q. (2011). An Improved Fast Ray Casting Volume Rendering Algorithm of Medical Image. *IEEE 4th International Conference on Biomedical Engineering and Informatics (BMEI)*.
- Liu, B., Wünsche, B. & Ropinski, T. (2010). Visualization by example – A constructive visual component-based interface for direct volume rendering, *Computer Graphics Theory and Applications*, 254-259.
- Liu, H., Yu, X., Wan, W. & Swaminathan, R. (2012). An Improved Spectral Subtraction Method. *International Conference on Audio, Language and Image Processing (ICALIP)*. 16-18 July, Page(s): 790 – 793.
- Lladó, X., Oliver, A., Cabezas, M., Freixenet, J., Vilanova, J.C., Quiles, A., Valls, L., Ramió-Torrentà, L. & Rovira, A. (2012). Segmentation of multiple sclerosis lesions in brain MRI: A Review of Automated Approaches. *Information Sciences* 186 (2012) 164–185.

- Lorensen, W.E. & Cline, H.E. (1987). Marching cubes: A High Resolution 3-D Surface Construction Algorithm. *Computer Graphics*. Volume 21, Number 4.
- Lundström, C. (2007). Efficient Medical Volume Visualization, Linköping Studies in Science and Technology Dissertations, No. 1125.
- Lv, X., Gao, X. & Zou, H. (2008). Interactive curved planar reformation based on snake model. *Comput Med Imaging Graph* 32(8):662–669.
- Ma, J., Murphy, D. & O’Mathuna, C. (2012). Visualizing Uncertainty in Multi-Resolution Volumetric Data Using Marching Cubes. *Proceedings of the International Working Conference on Advanced Visual Interfaces*, ACM New York, NY, USA, pp. 489-496.
- Manke, F. & Wönsche, B. (2008). A Direct Volume Rendering Framework for the Interactive Exploration of Higher-Order and Multifield Data. *GRAPP – International Conference on Computer Graphics Theory and Applications*.
- Manke, F. & Wünschev, B. (2009). Texture-Enhanced Direct Volume Rendering. *GRAPP- International Conference on Computer Graphics Theory and Applications*.
- Marner, L., Nyengaard, J. R., Tang, Y. & Pakkenberg, B. (2003). Marked loss of Myelinated Nerve Fibers in the Human Brain with Age. *Journal of Comparative Neurology*. 462:144–152. [PubMed: 12794739].
- Martin, J.P., Vickery, R.J., Ziegeler, S. & Angelini, R. (2010). SSH Enabled ParaView. *DoD High Performance Computing Modernization Program Users Group Conference*. IEEE.
- Martin, K., Ibáněz, L., Avila, L., Barré, S. & Kaspersen, J.H. (2005). Integrating Segmentation Methods from the Insight Toolkit into A Visualization Application. *Medical Image Analysis* 9, 579–593.
- Max, N. (1995). Optical Models for Direct Volume Rendering. *IEEE Transactions on Visualization and Computer Graphics*, Vol.1, 99-108.

- McCormick, B.H., DeFanti, T.A. & Brown, M.D. (1987). Visualization in Scientific Computing, Computer Graphics Vol. 21, No 6, November, 1987.
- McManus, J.P. & Kinsman, C. (2002). *C# Developer's Guide to ASP .NET, XML, and ADO .NET*: Addison-Wesley, New York.
- Meißner, M., Pfister, H., Westermann, R. & Wittenbrink, C.M. (2000). Volume Visualization and Volume Rendering Techniques. The Euro Graphics Association.
- Mensmann, J., Ropinski, T. & Hinrichs, K. (2010). An advanced volume raycasting technique using GPU stream processing. *Computer Graphics Theory and Applications*, page 190-198.
- Mensmann, J., Ropinski, T. & Hinrichs, K. (2010). An Advanced Volume Raycasting Technique using GPU Stream Processing. *International Conference of Computer Graphics Theory Appl.*, 2010, pp. 190–198.
- Merck, D. (2009). *Model Guided Rendering for Medical Images*, University of North Carolina at Chapel Hill.
- Metropolis, N., Rosenbluth, A., Rosenbluth, M., Teller, A. & Teller, E. (1953). Equation of State Calculations by Fast Computing Machines. *Journal of Chem. Physics*, 21: 1087– 1092.
- Meißner, M., Huang, J., Bartz, D., Mueller, K. & Crawfis, R. (2000). A Practical Evaluation of Popular Volume Rendering Algorithms: *IEEE/ACM. Symposium on Volume Visualization*, Salt Lake City, Utah.
- Mohamed, M.A., Abdul-Fattah, A.F.A, Asem, A.S., & El-Bashbishy, A.S. (2011). Medical image filtering, fusion and classification Techniques. *Egyptian Journal of Bronchology*. Vol. 5, No 2.
- Moreland, K. (2008). *The ParaView Tutorial*. Sadia National Laboratories, United States.

- Moreland, K., Ayachit, U., Geveci, B. & Ma, K. -L. (2011). Dax Toolkit: A Proposed Framework for Data Analysis and Visualization at Extreme Scale. IEEE Symposium on Large Data Analysis and Visualization (LDAV). pp.: 97 – 104.
- Moulik, S. & Boonn, W. (2011). The Role of GPU Computing in Medical Image Analysis and Visualization. Medical Imaging, 2011. Advanced PACS- based Imaging informatics and Therapeutic Applications. Proc. of SPIE Vol. 7967, 79670L.
- Mueller, K., Chen, M. & Kaufman, A. (2001). Volume Graphics', (Eds.) Springer. London.
- Muigg, P., Hadwiger, M., Doleisch, H., & Gröller, E. (2011). Interactive Volume Visualization of General Polyhedral Grids. IEEE Transactions on Visualization and Computer Graphics, Vol. 17, no.12.
- Nakajima, H., Hasegawa, K., Nakata, S. & Tanaka, S. (2009). Volume Visualization with Grid-Independent Adaptive Monte Carlo Sampling. Fifth International Conference on Intelligent Information Hiding and Multimedia Signal Processing. IHH-MSP. Pp. 1301-1304.
- Ng, K. -W., Wong, H.-C., Wong, U.-H. & Pang, W.-M. (2010). Probe-Volume: An Exploratory Volume Visualization Framework. 23rd International Congress on Image and Signal Processing (CISP). Vol. 5, pp. 2392 – 2395.
- Nickolls, J., Buck, I., Garland, M. & Skadron, K. (2008). Scalable Parallel Programming with CUDA. ACM Queue, 6(2):40–53.
- Nowak, R.D. (1999). Wavelet-Based Rician Noise Removal for Magnetic Resonance Imaging. IEEE Trans Image Process 8(10):1408–1419.
- Ohtake, Y., Belyaev, A., Alexa, M., Turk, G. & Seidel, H.-P. (2003). Multi-Level Partition of Unity Implicits, ACM Transactions on Graphics, Vol. 22, No.2 (2003) pp. 463-470.
- Oiso, M., Yasuda, T., Ohkura, K. & Matumura, Y. (2011). Accelerating Steady-State Genetic Algorithms based on CUDA Architecture. Congress on Evolutionary Computation (CEC), IEEE. Pp. 687 – 692, New Orleans, LA.



- Othman, M.F., Abdulahi, N. & Ahmad Rusli, N.A. (2010). An Overview of MRI Brain Classification Using FPGA Implementation, IEEE Symposium on Industrial Electronics and Applications.
- Owen, S. (1993). Visualization Education in the USA. *Journal of Computers and Education*. Vol. 8, pp. 339-345, 1993.
- Paulinas, M. & Usinskas, A. (2007). A survey of genetic Algorithms applications for image enhancement and segmentation”, *Information Technology Control*, Vol. 36, No. 3, pp. 278-284.
- Pelt, R.V., Vilanova, A. & Wetering, H.V.D. (2010). Illustrative Volume Visualization Using GPU-Based Particle Systems. *IEEE Transactions on Visualization and Computer Graphics*, Vol. 16, Issue: 4, pp. 571-582.
- Peng, Y., Dong, J., Chen, L., Chu, H. & Yong, J. (2011). An Optimal Color Mapping Strategy based on Energy Minimization for Time-varying Data. *212th International Conference on Computer-Aided Design and Computer Graphics (CAD/Graphics)*, pp. 411- 417.
- Perona, P. & Malik, J. (1990). Scale-space and edge detection using anisotropic diffusion, “*IEEE Trans. Pattern Anal. Mach. Intell.*, Vol. 12, No. 7, pp629 – 639.
- Petrescu, L., Morar, A., Moldoveanu, F. & Asavei, V. (2011). Real Time Reconstruction of Volumes from Very Large Datasets Using CUDA. *15th International Conference on System Theory, Control, and Computing (ICSTCC)*, pp. 1-5.
- Pham, D., Xu, C. & Prince, J. (2000). Current methods in medical image segmentation. *Annual Review of Biomedical Engineering*, vol. 2, pp. 315– 337.
- Ponraj, D.N., Jenifer, M.E., Poongodi, P. & Manoharan, J.S. (2011). A Survey On the Preprocessing Techniques of Mammogram for the Detection of Breast Cancer. *Journal of Emerging Trends in Computing and Information Sciences*. Vol. 2, No. 12, ISSN 2079-8407.

- Porter, T. & Duff, T. (1984). Compositing Digital Images: *Computer Graphics*, vol. 18, no. 3.
- Praßni, Jörg-Stefan., Ropinski, T. & Hinrichs, K. (2010). Uncertainty-Aware Guided Volume Segmentation. *IEEE Transactions on Visualization and Computer Graphics*, Vol. 16, no. 6.
- Pu, J., Leader, J.K., Zheng, B., Knollmann, F., Fuhrman, C., Scieurba, F.C., Gur, D. (2009). A Computational Geometry Approach to Automated Pulmonary Fssure Segmentation in CT Examinations. *IEEE Transaction Medical Imaging* 28(5): pp. 710–9.
- Qin, A.K., Raimondo, F., Fobes, F. & Ong, Y.S. (2012). An Improved CUDA-Based Implementation of Differential Evolution on GPU. *ACM Genetic and Evolutionary Computation Conference. GECCO*, Philadelphia, USA.
- Qu, D., Luo, Y. & Tan, W. (2011). An Improved Painting-Based Transfer Function Design Approach with CUDA-Acceleration. *IEEE International Conference on Computer Science and Automation Engineering (CSAE)*. Pp 372-377.
- Qureshi, M.N.I., Lee, J.-E., & Lee, S.W. (2012). Robust Classification Techniques for Connection Pattern Analysis with Adaptive Decision Boundaries Using CUDA. *IEEE International Conference on Cloud Computing and Social Networking (ICCCSN)*.
- Rodallec, M.H., Marteau, V., Gerber, S., Desmottes, L. & Zins, M. (2008). Craniocervical arterial dissection: spectrum of imaging findings and differential diagnosis, *Radiographics* 28:1711– 1728.
- Roos, J.E., Fleischmann, D., Koechl, A., Rakshe T., Straka M., Napoli, A., Kanitsar, A., Sramek, M., & Groeller, E. (2007). Multipath curved planar reformation of the peripheral arterial tree in CT angiography, *Radiology* 244:281–290.
- Rosenblum, L., Earnshaw, R.A., Encarnacao, J., Hagen, H. A., Kaufman, S.K., Nelson, G., Post, F. & Thalmann, D. (1994). *Scientific Visualization: Advances and Challenges*, Academic Press.

- Ross, J.C., Estepar, R., Kindlman, G., Dfaz, A., Westin, C.F., Silverman, E.K. Washko, G.R. (2010). Automatic Lung Lobe Segmentation using Particles, Thin Plate Splines and Maximum A Posteriori Estimation. *Med Image Comput-Assist Intervent* 2010:163–71.
- Sabella, P. (1988). A Rendering Algorithm for Visualizing 3D Scalar Fields: *Computer Graphics*. Volume 22, Number 4.
- Sakamoto, N. & Koyamada, K. (2005). Particle Generation from User- Specified Transfer Function for Point-Based Volume Rendering. *IEEE Visualization Proceedings Compendium*: 125-126.
- Sanftmann, H.,Cipriani, N. & Weiskopf, D. (2011). Distributed Context-Aware Visualization. *IEEE International Conference on Pervasive Computing and Communications Workshops (PERCOM Workshops)*. Pp. 251 – 256.
- Schroeder, W., Martin, K. & Lorensen, B. (2002). *The visualization Toolkit, An object-oriented approach to 3D graphics*, 3rd Edition, Pearson Education, Inc.
- Senthikumar, N. & Rajesh, R. (2008). A Study of Split and Merge for Region Based Image Segmentation. *Proceedings of UGC sponsored National conference network security (NCNS-08)*, 2008, pp.57-61.
- Senthilkumarn, N. & Rajesh, R. (2009). Edge Detection Techniques for Image Segmentation - A Survey of Soft Computing Approaches. *IJRTE*, Vol 1, No2, 250-254.
- Sethian, J. A. (1999). *Level Set Methods and Fast Marching Methods: Evolving Interfaces in Computational Geometry*. Fluid Mechanics. Computer Vision, and Materials. Cambridge University Press, 2 Edition.
- Sha, D.D. & Sutton, J.P. (2001). Towards automated enhancement, segmentation and classification of digital brain images using networks of networks, *Inf. Sci.* 138 (1–4) (2001) 45–77.

- Shabaneh, N., Amirpour, S., Stafford, S. & Shirazi, N. (2004). Radiation Health Risks and Benefits. *Computed Tomography*.
- Shen, A. & Luo, L. (2008). Point-Based Digitally Reconstructed Radiograph. *Proc. Int. Conf. Pattern Recog.*, 2008, pp. 1–4.
- Shen, H-W., & Johnson, C. (1994). Differential Volume Rendering: A Fast Volume Visualization Technique for Flow Animation. *Proceedings of the Visualization '94 Conference*, October 1994, pp. 180-187.
- Shi, X., Li, C., Wang, X. & Li, K. (2009). A Practical Approach of Curved Ray Prestack Kirchhoff Time Migration on GPGPU. *Advanced Parallel Processing Technologies 8th International Symposium*, pp. 165–176.
- Shihao, C., Guiqing, H. & Chongyang, H. (2009). Rapid Texture-Based Volume Rendering, *International Conference on Environmental Science and Information Application Technology*.
- Shihao, C., Guiqing, H. & Chongyang, H. (2009). Interactive GPU-based volume rendering for medical image, *Biomedical Engineering and Informatics, BMEI*.
- Siddique, M.T. & Zakaria, M.N. (2010). 3D Reconstruction of geometry from 2D image using Genetic Algorithm. *IEEE International Symposium in Information Technology (ITSim)*, Volume : 1, on page(s): 1 – 5, ISSN : 2155- 897, Print ISBN: 978-1-4244-6715-0.
- Sijbers, J., Dekker, A.J.D., Audekerke, J.V., Verhoye, M. & Dyck, D.V. (1998) Estimation of the noise in magnitude MR images. *Magnetic Resonance Imaging* 16(1):87–90.
- Song, J., Liu, Y., Gewalt, S.L., Cofer, G. & Johnson, G.A. (2009). Least-Square NUFFT Methods Applied to 2-D and 3-D Radially Encoded MR Image Reconstruction. *IEEE Transactions On Biomedical Engineering*, Vol. 56, No. 4, April 2009.
- Sonka, M. & Fitzpatrick, J.M. (2000). *Handbook of Medical Imaging*. SPIE.

- Speray, D. & Kennon, S. (1990). Volume probes: interactive data exploration on arbitrary grids. *SIGGRAPH Comput. Graph*, 24(5): 5-12.
- Styner, M., Lee, J., Chin, B., Chin, M., Commowick, O., Tran, H., Jewells, V. & Warfield, S. (2008). 3D Segmentation in the Clinic: A Grand Challenge II: MS Lesion Segmentation. *Grand Challenge Work.: Mult.Scler.Lesion Segm. Challenge*, pp. 1–8.
- Subhranil Koley, S. & Majumder, A. (2011). Brain MRI Segmentation for Tumor Detection using Cohesion based Self Merging Algorithm. *IEEE 3rd International Conference on Communication Software and Networks (ICCSN)*. Page(s): 781 – 785.
- Sun, Y., Bhanu, B. & Bhanu, S. (2009). Symmetry Integrated Injury Detection for Brain MRI, *Image Processing (ICIP), 16th IEEE International*, Pages 661 – 664.
- Suter, S.K., Zollikofer, C.P. & Pajarola, R. (2010). Application of Tensor Approximation to Multiscale Volume Feature Representations. *Proc. Vision, Modeling and Visualization*, pages 203–210.
- Suter, S.K., Gutiérrez, J.A.I., Marton, F., Agus, M., Elsener, A., Zollikofer, C.P.E., Gopi, M., Gobbetti, E. & Pajarola, R. (2011). Interactive Multiscale Tensor Reconstruction for Multiresolution Volume Visualization. *IEEE Transactions on Visualization and Computer Graphics*, Vol. 17, No. 12.
- Szirmay-Kalos, L., Umenhoffer, T., Tóth, B. & Szécsi, L. (2010). Volumetric Ambient Occlusion for Real-Time Rendering and Games. *IEEE Computer Graphics and Applications*, Volume: 30, Issue: 1, Pp. 70-79.
- Tan, S., Yang, J. & Sun, W. (2011). Internet-Based Platform for Power System Simulating and Planning: *Second International Conference on Mechanic Automation and Control Engineering (MACE)*, IEEE.
- Tanoori, B., Azimifar, Z., Shakibafar, A. & Katebi, S. (2011). *Computers in Biology and Medicine* 41 (2011) 619–632.

- Tawara, T. & Ono, K. (2010). A Framework for Volume Segmentation and Visualization Using Augmented Reality. IEEE Symposium on 3D User Interfaces (3DUI).
- Teo, P.C. & Heeger, D.J. (1994). Perceptual image distortion: Proc. 1<sup>st</sup> International Conference on Image Processing, pp. 982-986.
- Teyseyre, A.R. & Campo, M.R. (2009). An Overview of 3D Software Visualization. IEEE Transactions on Visualization and Computer Graphics, Vol. 15, No. 1.
- The first Information Visualization Symposium (InfoVis) (1995). IEEE Computer Society Press, Los Alamitos, CA.
- The Oxford English Dictionary (1989). Oxford Advanced Learner's Dictionary of Current English, Oxford University Press, Second Edition.
- Tornai, G.J. & Cserey, G. (2010). 2D and 3D Level-Set Algorithms on GPU: 2010 12th International Workshop on Cellular Nanoscale Networks and their Applications (CNNA), IEEE.
- Tsai, Y.-T. & Shih, Z.-C. (2006). All-Frequency Precomputed Radiance Transfer using Spherical Radial Basis Functions and Clustered Tensor Approximation. ACM Transactions on Graphics, 25(3):967–976.
- Van, R.E.M, De, H.B., Van, D.V.S., Prokop, M. & Van, G.B. (2009). Automatic Segmentation of Pulmonary Segments from Volumetric Chest CT Scans. IEEE Trans Med Imaging 2009;28(4):621–30.
- Vawter, C. & Roman, E. (2001). J2EE vs. Microsoft.NET A comparison of building XML-based web services: Prepared for Sun Microsystems, Inc.
- VenuGopal, T. & Naik, P.P.S. (2011). Image Segmentation and Comparative Analysis of Edge Detection Algorithms. Int. Journal of Electrical, Electronics & Computing Technology, Vol.1 (3).ISSN 2229-3027.
- Vivekanandan, D. & Raj, S.R. (2011). A Feature Extraction Model for Assessing the Growth of Lung Cancer in Computer Aided Diagnosis IEEE-International Conference on Recent Trends in Information Technology, MIT, Anna University, Chennai.

- Wakid, M., Kirmizibayrak, C. & Hahn, J.K. (2011). Texture Mapping Volumes using GPU-Based Polygon-Assisted Raycasting. IEEE 16th International Conference on Computer Games. Page(s): 162 – 166.
- Walter, T., Shattuck, D.W., Baldock, R., Bastin, M.E., Carpenter, A.E., Duce, S., Ellenberg, J., Fraser, A., Hamilton, N., Pieper, S., Ragan, M.A., Schneider, J.E., Tomancak, P. & Hériché, Jean-Karim (2010). Visualization of image data from cells to organisms” S26, Vol.7 No.3s, Nature Methods Supplement.
- Wang, L., Zhang, Y. & Feng, J. (2005). On the Euclidean Distance of Images. IEEE Transactions On Pattern Analysis and Machine Intelligence, Vol. 27, No. 8.
- Wang, R., Wan, W., Ma, X., Wang, Y. & Zhou, X. (2011). Accelerated Algorithm for 3D Intestine Volume Reconstruction Base on VTK. IEEE International Conference on Audio Language and Image Processing (ICALIP), pp: 448 – 452, Print ISBN: 978-1-4244-5856-1.
- Wang, S.Q., Zhang, J.H. & Yao, Z.X. (2009). Accelerating 3D Fourier Migration on Graphics Processing Units. SEG Expanded Abstracts, pp. 3020–3024.
- Węgliński, T. & Fabijańska, A. (2011). Brain Tumor Segmentation from MRI Data Sets using Region Growing Approach. MEMSTECH11, 11-14 May 2011, Polyana-Svalyava (Zakarpattya), Ukraine.
- Weiler, M., Westermann, R., Hansen, C., Zimmerman, K. & Ertl, T. (2000). Level-of-Detail Volume Rendering via 3d Textures. Proceedings of Symposium on Volume Visualization, pages 7–13. ACM, SIGGRAPH.
- Wen, X.B., Zhang, H. & Jiang, Z.T. (2008). Multiscale Unsupervised Segmentation of SAR Imagery using the Genetic Algorithms. Sensors, Vol.8, pp.1704-1711.
- Williams, A., Barrus, S., Morley, R.K. & Shirley, P. (2005). An Efficient and Robust Ray-Box Intersection Algorithm. Journal of Graph., GPU Game Tools, Vol. 10, no. 1, pp. 49–54, 2005.

- Williams, D., Grimm, S., Coto, E., Roudsari, A. & Hatzakis, H. (2008). Volumetric curved planar reformation for virtual endoscopy. *IEEE Trans Vis Comput Graph* 14(1):109–119.
- Winter, A.S. (2002). *Field-based Modelling and Rendering*. University of Wales, Swansea. PhD thesis.
- Wong, H.C., Wong, U.H. & Tang, Z.S. (2009). Direct volume rendering by transfer function morphine. The 7th International Conference on Information Communications and Signal Processing (ICICS), Beijing, China, pp. 1-4.
- Wu, D., Tian, H., Hao, G., Du, Z. & Sun, L. (2010). Design and Realization of an Interactive Medical Images Three Dimension Visualization System. *IEEE 3rd Internaltional Conference on Biomedical Engineering and Informatics (BMEI)*.
- Wu, Q., Xia, T., Chen, C., Lin, H.-Y.S., Wang, H. & Yu, Y. (2008). Hierarchical Tensor Approximation of Multidimensional Visual Data. *IEEE Transactions on Visualization and Computer Graphics*, 14(1):186–199.
- Wu, Y. (2006). *Effective, Intuitive and Intelligent Volume Visualization*, Department of Computer Science, Hong Kong University of Science and Technology.
- Xiao, Y., Chen, Z. & Zhang, L. (2009). Accelerated CT Reconstruction Using GPU SIMD Parallel Computing with Bilinear Warping Method: The 1<sup>st</sup> International Conference on Information Science and Engineering (ICISE), IEEE.
- Xie, K., Yu, W., Yu, H., Wu, P., Li, T. & Peng, M. (2011). GPU-based Multi-Resolution Volume Rendering for Large Seismic Data. *IEEE International Conference on Intelligence Science and Information Engineering*, pp. 245 - 248.
- Xujia, Q., Sida, Z., Xinhong, C. & Jun, H. (2009). Research and implementation of multi-dimensional transfer fucntion based on boundaries, *Biomedical Engineering and Informatics*.



- Yang, Guang-Zhong & Firmin, D.N. (2000). The birth of the first CT scanner. *Engineering in Medicine and Biology Magazine, IEEE*. Volume: 19 , Issue:1 pp: 120 – 125, ISSN : 0739-5175.
- Yang, X., Sechopoulos, I. & Fei, B. (2011). Automatic Tissue Classification for High-resolution Breast CT Images Based on Bilateral Filtering. *Proceedings Vol. 7962. Medical Imaging 2011: Image Processing, ISBN: 9780819485045.*
- Yeo, B.-L., & Liu, B. (1995). Volume rendering of DCT-based compressed 3D Scalar Data. *IEEE Transactions on Visualization and Computer Graphics*, 1(1):29–43.
- Yun, Y. & Xing, Z. (2010). An improved Method for volume rendering. 2nd International Symposium on Information Engineering and Electronic Commerce (IEEC), Issue Date : 23-25 July 2010, On page(s): 1 – 3.
- Zhang, F. & Ma, L. (2010). MRI Denoising Using the Anisotropic Coupled Diffusion Equations. *IEEE 3rd International Conference on Biomedical Engineering and Informatics (BMEI 2010).*
- Zhang, Z. -M., Lu, W., Shi, Y.-Z., Yang, T.-L. & Liang, S.-L. (2012). An Improved Volume Rendering Algorithm Based on Voxel Segmentation. *IEEE International Conference on Computer Science and Automation Engineering (CSAE), Vol.1, pp. 372 – 375.*
- Zhang, Q., Eagleson, R. & Peters, T.M. (2007). Rapid Voxel Classification Methodology for Interactive 3D Medical Images Visualization. *The 10th International Conference on Medical Image Computing and Computer Assisted Intervention (MICCAI), Brisbane, Australia, pp 86-93.*
- Zhang, Q., Eagleson, R. & Peters, T.M. (2010). A Technical Overview with a Focus on Medical Applications, *Journal of Digital Imaging.*
- Zhao, F. & McGinnity, T.M. (2011). A Low-cost Real-time Three-dimensional Confocal Fluorescence Endomicroscopy Imaging System. *IEEE International Conference on Healthcare Informatics, Imaging and Systems Biology, pp. 126 – 133.*

- Zheng, Z., Xu, W. & Mueller, K. (2010). VDVR: Verifiable Visualization of Projection-Based Data. *IEEE Transactions on Visualization And Computer Graphics*, Vol. 16, NO. 6, pp. 1515 – 1524.
- Zhou, H., Tao, Y., Lin, H., Dong, F. & Clapworthy, G. (2011). Shape-Enhanced Maximum Intensity Projection. *Springer-Verlag Vis Comput* 27: 677–686.
- Zhu, Y., Ma, X., Zhou, X., Sun, Y., Yang, W., Zhang, S. & Wang, W. (2011). Research of Medical Image Reconstruction System based-on MAC OS. *IEEE Conference on Smart and Sustainable City (ICSSC 2011)*. IET International. pp: 1 – 4, Print ISBN: 978-1-84919-326-9.
- Zitova, B. & Flusser, J. (2003). Image Registration Methods: A Survey. *Image and Vision Computing* 21 (2003), 977–1000.